Semaphorin 3A augments macrophage foam cell migration

Vincent Ta

Department of Experimental Medicine

Faculty of Medicine

McGill University, Montreal

Submitted July 2019

A thesis submitted to McGill University in partial fulfillment of the requirements of the degree of Master of Science

© Vincent Ta, 2019

Table of Contents

Abstract (English)	4
Résumé (français)	5
Acknowledgements	
Contribution of authors	8
Introduction	10
List of abbreviations	
1. Literature review	
1.1. Atherosclerosis	
1.1.1. Overview of atherosclerosis	
1.1.2. Biomechanical basis of atherosclerosis.	
1.1.3. Role of lipids and monocytes in the initial formation of atherosclerotic lesions	
1.1.4. Progression to advanced plaques	
1.1.5. The cholesterol hypothesis and atherosclerotic plaque regression	
1.2. Semaphorin 3A	
1.2.1. Overview of Semaphorins	
1.2.2. Action of Semaphorins in various systems	
1.2.3. Semaphorins in atherosclerosis	25
2. Hypothesis and aims	27
2.1. Hypothesis	
2.2. Research aims	27
3. Summary of previous work on Semaphorin 3A in atherosclerosis	28
4. Materials and methods	30
4.1. Plasmid information and bacterial preparation	
4.2. Cell line culture, plasmid transfections, and sample collection	
4.3. Mouse handling, high fat diet regimen, and electroporation protocol	31
4.4. Mouse euthanasia and sample collection	
4.5. Cryosectioning and tissue staining	
4.6. Extraction and culturing of primary bone marrow-derived monocyte-macrophages	
4.7. Bone marrow-derived macrophage trans-well migration assay	
4.8. Bone marrow-derived macrophage RhoA GTPase activation experiments	ker
analysis	
4.10. Western blots	
4.11. Statistical methods	
Table 1: List of antibodies used in experiments	4(
5. Results	
5.1. Transfected cells show no differences between groups by Western blot	
5.2. Electroporated quadriceps show distinct patterns between groups by Western blot	
5.3. Sema3A overexpression does not affect plaque size during regression, but appears to i	
a regression-induced increase in plaque collagen	44
5.4 Sama 3.4 induced M2 magraphage abametovic is mediated by Dho 4 signaling	
5.4. Sema3A-induced M2 macrophage chemotaxis is mediated by RhoA signaling	45

7.	Conclusion	54
8.	References	55

Abstract (English)

Background and hypothesis: Atherosclerosis is a disease involving the gradual buildup of lipids, fibrotic material, and inflammatory cells in lesions lining the arterial wall, which continually grow and can eventually block local circulation or rupture and form blood clots that cut off circulation elsewhere, culminating in life-threatening diseases such as heart attacks and stroke. Lifestyle modifications and statin drugs help to lower circulating lipids and mitigate these outcomes, but they may still occur nevertheless. Adopting a more mechanistically focused approach, our goal is to restore motility to the lipid-overloaded foam cells that become trapped inside atherosclerotic plaques and contribute to inflammation and rupture. We hypothesize that Sema3A, known to regulate cell motility in various contexts, can re-mobilize foam cells and induce plaque regression.

Methods: In vivo, ApoE^{-/-} mice on a high fat diet for nine weeks were returned to a chow diet and electroporated with plasmids containing Sema3A or GFP (as a control) to overexpress these proteins and then determine whether they affect plaque regression. In vitro, bone marrow- and peritoneum-derived macrophages and foam cells were extracted to test whether Sema3A affects their migration and expression of M1/M2 markers.

Results: Neither GFP nor Sema3A plasmid-treated mice had plaque regression. In vitro, however, Sema3A boosts M2 macrophage and foam cell chemoattraction towards MCP-1 through RhoA GTPase-ROCK signaling.

Conclusion: Due to the lack of plaque regression in the control condition, no conclusions can be made on the effect of Sema3A on plaque regression. However, Sema3A does increase M2 macrophage and foam cell motility, suggesting that it has the potential to boost foam cell egress from atherosclerotic lesions and result in regression.

Résumé (français)

Contexte et hypothèse: L'athérosclérose est une maladie se caractérisant par l'accumulation progressive de lipides, de fibres, et de cellules inflammatoires dans la paroi vasculaire des artères, conduisant à la formation de plaques. Celles-ci se développent au cours des années, peuvent obstruer le vaisseau, se rompre et provoquer ainsi la formation de caillots, qui peuvent bloquer la circulation sanguine, menant à des manifestations cliniques telles que l'infarctus du myocarde et les accidents vasculaires cérébraux. Les changements de mode de vie et les statines aident à abaisser la cholestérolémie et par conséquent le taux de morbidité et de mortalité associés aux évènements cardiovasculaires, mais ceux-ci peuvent encore se produire. En employant une stratégie plus ciblée au niveau mécanique, notre objectif est de rétablir la motilité des macrophages spumeux qui sont immobilisés dans la plaque après avoir accumulé un excès de lipides, contribuant à l'inflammation et à la rupture des plaques. Nous proposons l'hypothèse que Sema3A, qui est connu comme régulateur de la motilité cellulaire dans plusieurs contextes divers, pourrait aider ces cellules spumeuses à quitter la plaque et par conséquent à entraîner la régression des plaques athéromateuses.

Méthodes: Les souris ApoE^{-/-} sont soumises à un régime gras pendant neuf semaines, puis à un régime normal. Le plasmide contenant Sema3A ou GFP (comme contrôle) sont administrés par électroporation, dans le but de les surexprimer et déterminer s'ils peuvent provoquer la régression de la plaque. In vitro, les macrophages et les cellules spumeuses sont récupérées à partir de la moelle osseuse et du péritoine pour tester l'effet de Sema3A sur la migration et l'expression des marqueurs macrophagiques M1/M2.

Résultats: Ni le plasmide GFP ni le plasmide Sema3A ont provoqué la régression de la plaque chez les souris. Cependant, en culture Sema3A augmente la migration MCP-1-dépendante des

macrophages M2 et des cellules spumeuses, impliquant la voie de la signalisation GTPase RhoA-ROCK.

Conclusion: Dû à l'absence de régression dans la condition contrôle, aucune conclusion n'a pu être tirée concernant l'effet de Sema3A sur la régression des plaques athéromateuses. Néanmoins, Sema3A augmente la motilité des macrophages M2 et des cellules spumeuses, suggérant que cela pourrait potentiellement aider les cellules spumeuses à sortir des plaques

athéromateuses et entraîner la régression.

Acknowledgements

First and foremost, I would like to thank my supervisor, Dr. Stephanie Lehoux, for giving me the opportunity to work on this project in her lab, for her financial support, and for her constant guidance and directing of my experiments. I would also like to thank our lab manager, Dr. Talin Ebrahimian, for helping me to interpret and analyze my results, and particularly for teaching me how to perform the in vitro migration experiments and for setting up my flow cytometry panels. Next, I would like to thank our postdoctoral fellow, Dr. France Dierick, who helped me greatly with my mouse dissections, tissue sectioning, histological staining, and microscopic imaging. I would also like to thank our lab technicians, David Simon and Maria Kotsiopriftis, who taught me how to perform Western blots, qPCR, and the plasmid cloning and transfection experiments. Finally, I would like to thank our PhD student, Nicholas DiStasio, for our stimulating discussions and brainstorming about each other's projects.

Outside of our immediate lab, I would like to give special thanks to my academic advisor, Dr. Koren Mann, and to my thesis committee members, Dr. Andrew Mouland and Dr. Alexandre Orthwein, for taking the time to attend my annual progress meetings and provide me with insightful feedback and recommendations for my project. I would also like to thank the staff of the animal facility at the Lady Davis Institute for their constant vigilance and support of our animals throughout our experiments, as well as Christian Young from the flow cytometry lab for his expertise in flow cytometry and cell counting.

Contribution of authors

I (Vincent Ta) reviewed and synthesized the relevant literature in order to put this project into a meaningful context. I wrote the present thesis in its entirety, receiving some minor feedback and corrections from my supervisor, Dr. Stephanie Lehoux. Finally, I was partly or fully involved in carrying out all of the experiments and analyses described below, with training and guidance from several members of my lab.

Dr. Stephanie Lehoux is the lab's principal investigator and my thesis project supervisor. She provided me with feedback, guidance, and support throughout the entire project. Dr. Lehoux generated the hypothesis underlying this project and designed the experiments to be conducted. Moreover, she and Dr. France Dierick, a postdoctoral fellow in our lab, trained me to perform the mouse dissections and other in vivo techniques.

Dr. Dierick taught me how to perform whole tissue preparation, cryosectioning, and immunofluorescence staining of the tissue sections. She provided significant feedback and corrections in translating the abstract of this thesis to French. Finally, she and Dr. Talin Ebrahimian, our lab manager and research associate, helped me greatly in conducting the flow cytometry experiments and analyses.

Dr. Ebrahimian provided thorough guidance through my thesis project. Most notably, she taught me how to extract and culture bone marrow cells from mice, and to perform migration and stimulation experiments with these cells. She also taught me how to extract macrophages from the mouse peritoneal cavity. Dr. Ebrahimian designed the panel of fluorescent antibodies used to determine the M1/M2 phenotype of peritoneal macrophages. She and David Simon, our former lab technician, taught me proper cell culture technique.

David taught me how to clone our DNA plasmids into bacteria, to be amplified for the cell transfection and mouse electroporation experiments. He also taught me how to perform plasmid transfections into cells, cell and tissue homogenization for protein extraction, and Western blots. Our new lab technician, Maria Kotsiopriftis, provided me with helpful tips on Western blot and tissue staining techniques. Finally, Nick DiStasio, a PhD student in our lab, taught me how to quantitatively analyze my Western blot results, and he and Dr. Ebrahimian helped me to properly set up the microscope to capture my images.

Introduction

One of the ultimate goals in the treatment of atherosclerotic cardiovascular diseases is the stabilization and regression of lesions. Thus far, this has primarily been achieved through lifestyle changes (e.g. diet and exercise) and through the use of lipid-lowering statins. Though statins have resulted in significant reductions in cardiovascular morbidity and mortality, many patients are still at risk for experiencing relapses in heart attacks and other events, particularly those with a highly inflammatory profile. To address this, we have decided to focus on macrophage foam cells, the phagocytes that are recruited to atherosclerotic plaques with the goal of clearing the lipid contents, but instead get trapped inside due to impaired motility brought about by excess lipid loading, and subsequently contribute to the perpetuation of plaque inflammation and progression. Borrowing a well-characterized chemokine from the nervous system that plays a major role in cell motility, Sema3A, we hypothesize that Sema3A could result in plaque regression by helping to restore foam cell motility, thereby allowing these cells to leave the atherosclerotic plaques in which they are trapped. Our objectives are 1. To test the effect of Sema3A in vitro on macrophage and foam cell motility and phenotype, particularly with regards to the pro-inflammatory, classically activated (M1) vs. alternatively activated, antiinflammatory (M2) paradigm; and 2. To determine whether the overexpression of Sema3A in a murine model of atherosclerosis can induce plaque regression.

List of abbreviations

α-SMA alpha smooth muscle actin

ABC transporter adenosine triphosphate-binding cassette transporter

ANOVA analysis of variance

ApoB and ApoE apolipoprotein B and apolipoprotein E

Arg1 Arginase 1 BM bone marrow

BCA brachiocephalic artery
BSA bovine serum albumin
CAD coronary artery disease
CAM cell adhesion molecule

VCAM-1 vascular cell adhesion molecule-1 ICAM-1 intercellular cell adhesion molecule-1

CRP C-reactive protein

DAPI 4',6-diamidino-2-phenylindole

DC dendritic cell

DMEM Dulbecco's Modified Eagle Medium

EC endothelial cell ECM extracellular matrix

eGFP enhanced green fluorescent protein ELISA enzyme-linked immunosorbent assay

G-LISA GTPase enzyme-linked immunosorbent assay

FBS fetal bovine serum

FC foam cell

FH familial hypercholesterolemia

GAPDH glyceraldehyde 3-phosphate dehydrogenase

HDL high-density lipoprotein

HFD high-fat diet (or alternatively Western diet)

HMG-CoA reductase 3-hydroxy-3-methyl-glutaryl-coenzyme A reductase

HRP horseradish peroxidase

IL-4 interleukin-4

iNOS inducible nitric oxide synthase

LDL low-density lipoprotein

LDLR low-density lipoprotein receptor M0 uncommitted macrophages

M1 pro-inflammatory, classically activated macrophages

M2 anti-inflammatory, reparative, alternatively activated macrophages

M-CSF macrophage colony-stimulating factor MCP-1 monocyte chemoattractant protein 1

MMP matrix metalloproteinase

MOMA-2 monocyte + macrophage (marker)

Nrp1 neuropilin-1

OCT gel optimal cutting temperature gel

ORO Oil Red O

OxLDL oxidized low-density lipoprotein

P/S penicillin/streptomycin PBS phosphate-buffered saline

PFA Paraformaldehyde

qPCR quantitative polymerase chain reaction

ROCK Rho-associated protein kinase reactive oxygen species

Sema3A Semaphorin 3A (also known as Collapsin-1)

SMC smooth muscle cell SR scavenger receptor

TBST tris-buffered saline with Tween 20

TNF- α tumor necrosis factor-alpha

1. Literature review

1.1. Atherosclerosis

1.1.1. Overview of atherosclerosis

Atherosclerosis is a chronic inflammatory disease in which the gradual accumulation of excess circulating lipids and immune cells in the arterial wall produces lesions, called plaques, that progressively narrow the arterial lumina. While these plaques can remain clinically silent throughout the first several decades of life, their continual growth can eventually lead to the partial or complete blockage of the affected arterial segments, impairing circulation to downstream tissues. More importantly, they may become increasingly fragile and susceptible to rupturing over time; when this occurs, the release of plaque contents into the circulation triggers the rapid formation of blood clots, which can obstruct blood flow either immediately at the site of formation or elsewhere in the circulation following their dislodgement. This results in tissue death and is the main cause of life-threatening cardiovascular diseases such as heart attack and stroke^{1,2}.

1.1.2. Biomechanical basis of atherosclerosis

Atherosclerotic lesions begin to develop in childhood and have been detected in infants as early as 6 months³⁻⁸. They tend to form specifically at vascular transition points such as bifurcations, branch points, and curvatures, where the vessel deviates from a straight line and imposes an abrupt change the direction of blood flow⁹⁻¹⁷. As shown in Figure 1¹⁸, the flow divider experiences high levels of shear stress, the

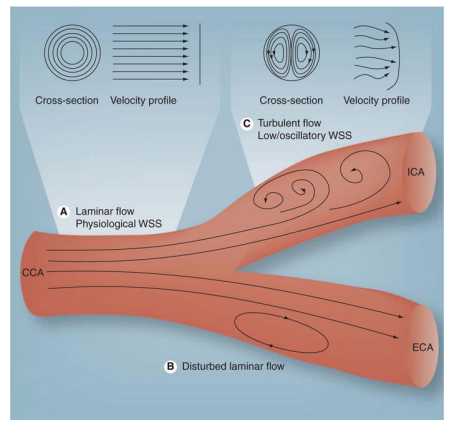


Figure 1¹⁸: The disruption of regular, laminar blood flow at vascular transition points serves as the biomechanical basis for the initial formation of atherosclerotic plaques.

frictional force between the stationary arterial wall and the blood flowing over it. High shear stress is associated with protection from atherosclerotic plaque development^{19,20}, although lesions can still form here in severe cases²¹⁻²⁴. On the opposite wall, blood flow separates laterally from the main stream, forming regions of reversed flow and low shear stress, which is associated with increased susceptibility to plaque development²⁵.

How do biomechanical factors predispose certain regions of the arteries to atherosclerosis? As the innermost cells in direct contact with blood flow, endothelial cells (ECs) are highly sensitive to mechanical stimuli such as changes in shear stress^{26,27}, which they can detect through surface mechanoreceptors and the cytoskeleton²⁸⁻³⁰. These signals influence the gene expression of ECs, allowing them to adaptively respond to hemodynamic changes³¹⁻³³. For example, cultured ECs exposed to low shear stress have increased surface expression of cell adhesion molecules (CAMs)^{8,34-39}, which permit the attachment of leukocytes. CAMs are also known to be induced under pro-inflammatory conditions⁴⁰⁻⁴³ such as during atherosclerosis. In vivo, the endothelium in regions of low shear stress has increased permeability, lipoprotein accumulation and oxidation, expression of CAMs, and recruitment of monocytes⁴⁴⁻⁴⁹, all of which promote the formation and progression of atherosclerotic lesions. Indeed, these are often the first places where advanced plaques will eventually form⁵⁰⁻⁵⁶.

1.1.3. Role of lipids and monocytes in the initial formation of atherosclerotic lesions Early on in life, long before the onset of any pathological changes, the intima (the innermost layer of arteries, which includes the endothelium along with the underlying extracellular matrix [ECM] and smooth muscle cells [SMCs]) undergoes an adaptive thickening in the

aforementioned susceptible regions of low shear stress, as a result of the non-uniform hemodynamic conditions that occur there⁵⁷. Physiologically, this helps to maintain vascular homeostasis by stabilizing blood flow velocity and preserving structural integrity^{50,58,59}. These thickened regions tend to collect low-density lipoprotein (LDL)^{60,61}, one of the main lipid carriers in the systemic circulation and a major component of plaques. Although there are low levels of LDL found in the healthy intima⁶², abundant lipoprotein accumulation is considered the initiating event in atherogenesis^{57,63-66}. In addition to increased endothelial permeability⁶⁷⁻⁷³, these vulnerable areas have increased lipoprotein retention^{63,64,66,74} through ionic interactions between the positively-charged apolipoprotein B (ApoB, the major protein scaffold component of LDL) and the negatively-charged proteoglycans in the intimal ECM⁷⁵.

Contrary to previous pathophysiological models⁷⁶, it is now understood that the progression of atherosclerosis does not simply involve a passive accumulation of lipids, but rather a complex inflammatory response in which various immune cells, particularly monocytes, are recruited in an attempt to remove LDL from the plaque. These phagocytes take up LDL via cell surface LDL receptors (LDLR), a process that is regulated by negative feedback: increases in intracellular cholesterol are detected by transcription factors called sterol regulatory element-binding proteins, which downregulate LDLR at the cell surface to help prevent excess LDL uptake⁷⁷⁻⁸⁰. In addition, high intracellular cholesterol levels upregulate ATP-binding cassette (ABC) transporters, namely ABCA1 and ABCG1^{81,82}. These proteins load cholesterol into high-density lipoprotein (HDL)⁸³⁻⁸⁵, the "good cholesterol" carrier which recirculates excess cholesterol from tissues back to the liver, where it can be eliminated through bile excretion⁸⁶.

At first glance, these mechanisms of limiting intracellular cholesterol accumulation seem to conflict with what is now recognized as a defining histological feature of atherosclerosis, the macrophage foam cell (FC), named after its characteristic lipid droplets (Figure 2⁸⁷) which store excess cholesterol taken up from their surroundings. Considering the negative feedback

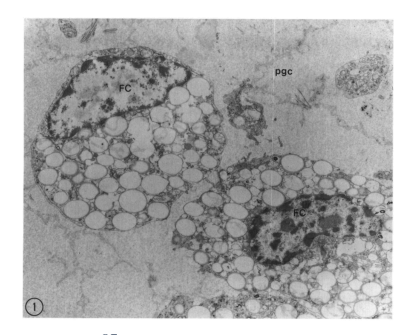


Figure 2⁸⁷: Transmission electron micrograph of foam cells, containing characteristic lipid droplets.

on cholesterol uptake, it was believed that FC formation would require an alternative pathway of LDL uptake that was independent of LDLR^{88,89}. Indeed, it is now known that LDL undergoes modifications, especially oxidation (OxLDL), in the intima⁹⁰, and is taken up through scavenger receptors (SRs) such as SR-A and SR-B (CD36)⁹¹. Unlike LDLR, SR-mediated uptake of modified LDL is not regulated by negative feedback, thereby permitting substantial intracellular LDL accumulation and FC formation^{77,92-95}.

As with low shear stress, OxLDL accumulation also activates the endothelium to express cell surface CAMs and chemokines involved in recruiting the circulating monocytes⁸⁹ that will eventually become FCs. First, monocytes begin rolling on the endothelial surface through interactions between monocytic P-selectin glycoprotein ligand-1 and endothelial P- and E-selectins⁹⁶⁻⁹⁸. Rolling is followed by firm adhesion, in which the monocytic integrins very late antigen-4 and lymphocyte function-associated antigen 1 bind endothelial vascular (VCAM-1) and intercellular cell adhesion molecules (ICAM-1), respectively^{99,100}. Next, monocytes cross the endothelial barrier into the underlying intimal space under the influence of chemokines such as monocyte chemoattractant protein-1 (MCP-1, also known as CCL2), CX₃CL1, and CCL5¹⁰¹⁻¹⁰⁵.

Finally, activated ECs release macrophage colony-stimulating factor (M-CSF), which promotes monocyte differentiation into macrophages⁸⁹ that begin engulfing lipids.

1.1.4. Progression to advanced plaques

FCs initially manifest as small, isolated cells in early atherosclerotic lesions that are invisible to the naked eye^{51,106,107}. Whereas leukocytes typically leave the affected tissue once inflammation has been resolved, the movement of FCs is encumbered by excess cholesterol loading¹⁰⁸⁻¹¹¹ and they have trouble exiting the plaque, instead accumulating inside the lesion and fueling chronic inflammation. In addition, the presence of OxLDL and other lipids in the arterial wall stimulates further monocyte recruitment and macrophage proliferation^{87,112-123}, gradually increasing the number of FCs until they eventually form visible fatty streak lesions¹⁰⁷.

High levels of intracellular OxLDL and cholesterol also promote macrophage apoptosis in atherosclerosis ¹²⁴⁻¹²⁹, for example by inducing endoplasmic reticulum stress ¹³⁰⁻¹³⁷. However, the phagocytosis of these apoptotic cells (mostly by other macrophages) is highly efficient in early lesions ¹³⁸⁻¹⁴⁰, so they do not accumulate to any significant degree. In fact, animal experiments suggest that this early-stage apoptosis impedes the progression of atherosclerosis ^{128,138,141-146}. In contrast, there is a much greater abundance of apoptotic macrophages found in later lesions. While this can be attributed in part to increased cell death, impaired phagocytosis has also been recognized to contribute to the accumulation of apoptotic cells in advanced plaques ^{139,147,148}. Like OxLDL, apoptotic antigens are also recognized by the scavenger receptors SR-A and SR-B. In this manner, the detection of apoptotic cells by phagocytic macrophages is limited by the presence of OxLDL, which can act as a competitive ligand as well as triggering the production of

anti-OxLDL antibodies that sequester the apoptotic antigens¹⁴⁹⁻¹⁵³. Furthermore, OxLDL can directly impair phagocytosis by altering actin polymerization^{153,154} or by causing cell membrane stiffening, preventing the formation of pseudopodia that are necessary for this process¹³⁹.

Eventually, the growing mass of lipids and apoptotic cells overwhelms the macrophages' phagocytotic capacity. These dying cells swell and burst open, releasing stored cell debris and lipids, along with pro-inflammatory cytokines that further perpetuate the recruitment of inflammatory cells¹⁵⁵⁻¹⁶⁷. At this point, the excess lipids begin to collect in extracellular pools that can disrupt the vascular structure, particularly that of the smooth muscle¹⁰⁷. Once they grow large enough, these lipid pools conglomerate into a necrotic core (Figure 3¹⁶⁸). SMCs are recruited from the media by



Figure 3¹⁶⁸: Cross-section of an atheroma and its characteristic lipid core.

necrotic and pro-inflammatory signals, producing collagen and forming a fibrous cap overlying the lipid core to contain and stabilize the lesion¹⁶⁹. Other common features of advanced plaques include calcification; surface fissures and ulcers, which can release lipids from deep within the plaque; hematomas and hemorrhages; and thrombotic deposits^{107,168}.

The most dangerous outcome for atherosclerotic plaques is for them to rupture and release their pro-inflammatory and pro-thrombotic contents into the circulation. This forms a thrombus that can cut off circulation either at the site of rupture or in smaller downstream arteries, such as the coronary arteries supplying the myocardium or the cerebral microvasculature, resulting in tissue death^{1,2}. Vulnerable plaques tend to have a large necrotic core, high macrophage content, and a thin fibrous cap with reduced collagen and SMC content^{168,170-172}. Plaques are most fragile at the

edges^{173,174} and particularly on the upstream side, a region of high shear stress. This suggests that while low shear stress plays a pivotal role in initial lesion formation, high shear stress promotes plaque rupture¹⁷⁵⁻¹⁷⁸. Indeed, high shear stress upregulates matrix metalloproteinases (MMPs), which degrade the fibrous cap¹⁷⁹. Interestingly, the pro-inflammatory milieu also stimulates the release of MMPs by macrophages¹⁸⁰. One of the ultimate goals in atherosclerosis research is to discover ways to pre-emptively impede, and perhaps even reverse lesion progression, so that these potentially life-threatening plaque ruptures can be avoided altogether.

1.1.5. The cholesterol hypothesis and atherosclerotic plaque regression

In the nineteenth century, Rudolf Virchow was one of the first to describe cholesterol and leukocyte accumulation in the arterial walls of patients who had succumbed to fatal heart attacks¹⁸¹. The idea that hypercholesterolemia plays a prominent role in atherosclerosis, commonly referred to as the cholesterol hypothesis, gained further support from experiments done by Ignatowski and Anitschkov, who observed plaque development in rabbits fed a high-fat diet (HFD)¹⁸²⁻¹⁸⁵. This went on to serve as an invaluable method for studying atherosclerosis in other animal models¹⁸⁶⁻¹⁸⁸. However, it was difficult to replicate this in mice, who mostly store cholesterol in HDL, resulting in low serum cholesterol and a naturally conferred resistance to atherosclerosis¹⁸⁹⁻¹⁹¹. Later, the advent of gene targeting technologies enabled the development of LDLR^{-/-192} and Apolipoprotein E knockout (ApoE^{-/-}) mice^{193,194}, the two most frequently used models today. These proteins are important in cellular lipid uptake, so their targeted deletion, in combination with HFD, accelerates plaque formation in mice, and has allowed this process to be studied within a much more reasonable time frame than in bigger animal models.

On the clinical side, large-scale longitudinal epidemiological studies such as the Framingham Heart Study^{195,196} and the Seven Countries Study¹⁹⁷ further reinforced the association between diets rich in saturated fats, the ensuing hypercholesterolemia, and coronary artery disease (CAD), warranting further research into the biochemistry of cholesterol. Through their work in patients with familial hypercholesterolemia (FH), American scientists Brown and Goldstein, who were the first to isolate and characterize LDLR, discovered that LDLR was mutated in FH and that this prevented cellular LDL uptake. The resulting drop in intracellular cholesterol promotes a compensatory upregulation in the activity of 3-hydroxy-3-methyl-glutaryl-coenzyme A (HMG-CoA) reductase, the rate-limiting enzyme in endogenous cholesterol biosynthesis. In collaboration with Akira Endo in Japan, they next inhibited HMG-CoA reductase in normal (non-FH) cells with the fungal compound Compactin, which conversely increased cell surface LDLR and LDL uptake¹⁹⁸⁻²⁰¹. In principle, then, targeting HMG-CoA reductase in vivo should promote LDL uptake from the surroundings (i.e. circulation); this idea was the impetus for the development of therapeutic HMG-CoA inhibitors, a class of drugs known today as statins.

Lipid lowering had previously been tested in animal models, which uncovered the phenomenon of plaque regression: lowering blood cholesterol, using strategies such as switching animals from a HFD to a chow diet over a prolonged period²⁰²⁻²⁰⁴, or by administering cholesterol-sequestering agents such as HDL²⁰⁵⁻²⁰⁷ or phosphatidylcholine²⁰⁸, decreases lesion size and macrophage/FC content, and stabilizes the fibrous cap by increasing collagen and SMC content^{189,209}. The hope with statins was to achieve the same outcome in humans. Indeed, the REVERSAL²¹⁰ & ASTEROID²¹¹ trials showed that intensive statin treatment results in plaque regression as

assessed by intravascular ultrasound, while the Scandinavian Simvastatin Survival Study (4S) found significantly reduced cardiovascular mortality after five years on Simvastatin²¹².

Despite the major impact that these drugs have had on cardiovascular medicine, statins are associated with several adverse events such as myopathies, increased incidence of diabetes mellitus, and liver toxicity²¹³. This has contributed to low adherence rates^{214,215}, putting patients at risk for the recurrence of cardiovascular disease^{216,217}. Furthermore, the recurrence of heart attacks among patients on statins is especially prominent in those with high levels of the proinflammatory marker C-reactive protein (CRP)^{218,219}, and in the recent CANTOS trial, an antibody-based immunotherapy targeting the pro-inflammatory cytokine IL-1β lowered recurrence and mortality rates in patients with elevated CRP²²⁰. Clearly, there is much to be gained by addressing factors beyond hypercholesterolemia. For example, FC egress from lesions is one of the first steps observed in plaque regression 188,221,222, so one approach would be to restore the impaired motility of these trapped FCs. Van Gils et al. found that neuronal guidance cues regulate the chemotaxis of macrophages in atherosclerosis²²³, and that these guidance cues are differentially expressed between the endothelia lining the inner and outer curvatures of the aortic arch²²⁴, which as previously stated have increased and decreased susceptibility to plaque formation, respectively. Among the signals they studied was one called Semaphorin 3A.

1.2. Semaphorin 3A

1.2.1. Overview of Semaphorins

The Semaphorins are a family of signaling proteins generally involved in regulating cell motility. Their functions have been thoroughly studied in the nervous system, particularly in the context of directing axon growth. The first Semaphorin identified was Fasciclin IV (Sema-1a), an axon guidance signal involved in the embryonic development of grasshoppers²²⁵. Around the same time, Collapsin-1 (Semaphorin 3A, Sema3A) was discovered in the developing chick brain²²⁶. It was named for its ability to induce the collapse of neurite growth cone structures, thereby restricting axon expansion to a single pre-programmed path.

There have been eight classes of Semaphorins identified thus far (Figure 4²²⁷): classes 1 and 2 in invertebrates, classes 3-7 in vertebrates, and class V in viruses^{228,229}. Semaphorins share several domains: an N-terminal export signal peptide, a highly conserved 500 amino acid-long Sema domain, an immunoglobulin-like domain, and a C-terminal basic tail²²⁶. While most Semaphorins bind Plexin receptors, class 3

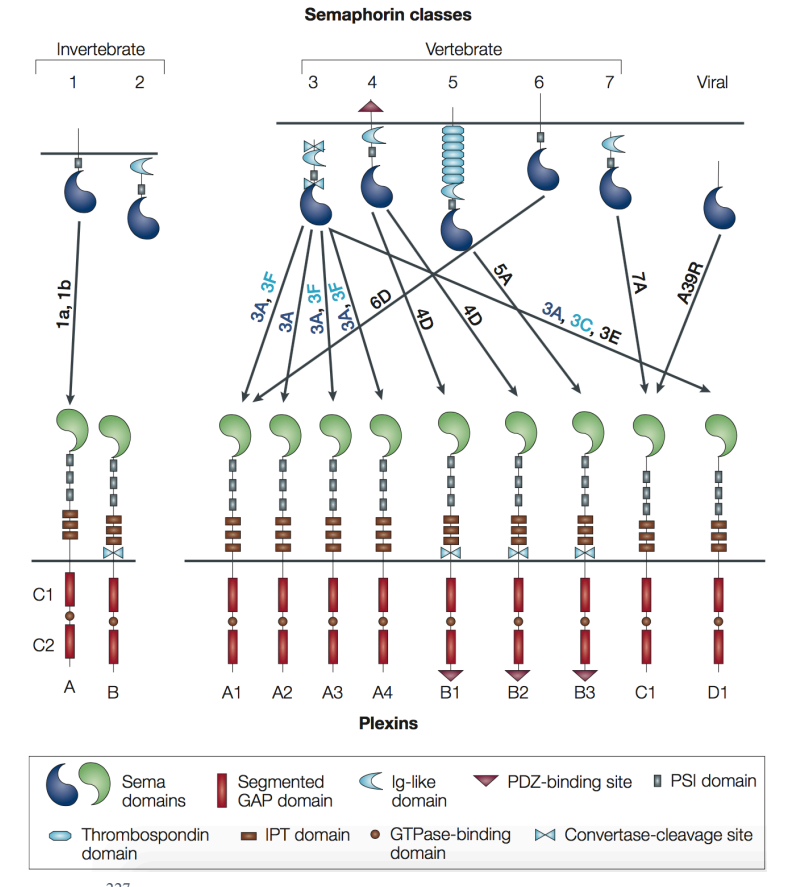


Figure 4²²⁷: Interactions between the different classes of Semaphorins and their Plexin receptors.

Semaphorins require an additional family of co-receptors, the Neuropilins²³⁰⁻²³². For the most part, their action in cell motility is mediated by the small Rho family of GTPases, which bind the intracellular tail of Semaphorin-activated Plexin receptors²²⁷. Rho GTPases direct polarized cell movement through cytoskeletal rearrangements, such as actin polymerization and actomyosin contraction, in conjunction with extracellular adhesion and detachment at the leading and trailing edges, respectively^{233,234}.

1.2.2. Action of Semaphorins in various systems

Semaphorins are best characterized for their role in the nervous system during embryonic development. Examples include directing neural crest cell migration towards the peripheral nervous system²³⁵ and repelling axon growth to prevent off-target synapsing²²⁹. Additionally, in adults they limit neuronal plasticity and regenerative capacity following injury²³⁶⁻²³⁸. Semaphorins have been implicated in many neurological disorders such as epilepsy^{239,240}, schizophrenia²⁴¹⁻²⁴⁴, Alzheimer's^{245,246}, Parkinson's disease^{247,248}, and multiple sclerosis²⁴⁹.

Semaphorins have been studied in other systems as well. Much like the branching structure of neural processes, proper vascular development also requires a delicate balance of signaling molecules. Class 3 Semaphorins disrupt the adhesion between adjacent ECs, allowing them to branch off from existing blood vessels²⁵⁰. Similar to its role in axon repulsion, Sema3A was found to direct vascular growth by stimulating ECs to secrete soluble flt1, a splice variant of vascular endothelial growth factor receptor that sequesters the ligand and limits angiogenesis²⁵¹. Semaphorins are also involved in cancer, generally as tumor suppressors^{227,252,253}. Sema3B and 3F are deleted in small-cell lung and other cancers^{254,255}, and reconstitution of these deleted

Semaphorins respectively induces cancer cell apoptosis^{256,257} and impaired metastasis^{250,258}, an example of cell movement. In bone remodeling, Sema3A suppresses bone-degrading osteoclasts²⁵⁹ and promotes bone deposition by inducing osteoblast formation^{260,261} and sensory innervation, which is known to affect bone homeostasis²⁶²⁻²⁶⁴.

However, most relevant to atherosclerosis is the role that Semaphorins play in the immune system, particularly in immune cell migration. Sema3A blocks dendritic cell (DC) antigen presentation to T cells. This has a delayed onset with respect to the initial cell-cell contact, so it is thought to terminate DC-mediated T cell activation²⁶⁵. Similarly, Sema3A disrupts interactions between thymic ECs and thymocytes, allowing these precursor T cells to exit the thymus and to complete their maturation²⁶⁶. Sema3A-Plexin A1 signaling is required for DC transmigration into the lymphatics by activating actomyosin contraction at the trailing edge (i.e. tail retraction), and inhibition of Rho-associated protein kinase (ROCK) abrogates this effect²⁶⁷, further implicating Rho GTPases as mediators of Sema-induced cell motility. T cells in patients with rheumatoid arthritis have reduced Sema3A and increased Neuropilin-1 (Nrp1) expression, and conversely, administering Sema3A suppresses inflammation in a mouse model of autoimmune arthritis²⁶⁸. Sema3A is also required for the resolution of cardiac inflammation following myocardial infarction, as Sema3A-deficient mice have prolonged leukocyte retention in the inflamed tissue²⁶⁹. In general, Sema3A seems to have anti-inflammatory properties, suggesting that it could have a protective effect against atherosclerosis.

1.2.3. Semaphorins in atherosclerosis

Several Semaphorins have been studied in mouse models of atherosclerosis. Compared to LDLR^{-/-} mice on HFD, LDLR^{-/-} Sema4D^{-/-} mice have reduced dyslipidemia-induced platelet hypersensitivity (e.g. adhesion to the endothelium, secretion of pro-inflammatory cytokines), which is known to be pro-atherogenic, and consequently have diminished plaque growth²⁷⁰. ApoE^{-/-} Sema4D^{-/-} mice also have less intimal neovascularization and plaque formation than ApoE^{-/-} mice, proposedly by limiting macrophage infiltration and the production of reactive oxygen species (ROS)²⁷¹. Macrophages isolated from an aortic transplant model of plaque regression^{272,273} have reduced expression of Sema3E compared to macrophages from progressing plaques, and in vitro migration experiments revealed that Sema3E blunts macrophage migration towards the regression-associated chemoattractant CCL19, again through signaling pathways involving Rho GTPases (Rac1 and Cdc42)²⁷⁴. ApoE^{-/-} Sema7A^{-/-} mice have reduced plaque formation compared to ApoE^{-/-} mice, and Sema7A is more highly expressed on the vulnerable inner curvature of the aortic arch than on the protected outer curvature²⁷⁵.

However, not all Semaphorins are associated with increased atherosclerosis. The same group that studied Sema7A²⁷⁵ also found that compared to the descending aorta, the relatively vulnerable aortic arch has reduced expression of several other Semaphorins, namely Sema3A. In agreement with this, Van Gils et al.²²⁴ looked at aortic arch EC expression of an array of common neuronal guidance cues during early atherosclerosis, and found reduced expression of Sema3A in ECs from the inner curvature compared to the outer curvature. This was further substantiated by in vitro experiments in which ECs exposed to atherogenic oscillatory flow had reduced expression of Sema3A compared to laminar flow. Functionally, they found that Sema3A impedes monocyte

migration towards the pro-atherogenic chemokine CCL2 and disrupts monocyte adhesion to human coronary ECs activated with tumor necrosis factor-alpha (TNF- α).

Based on its anti-inflammatory properties and the above findings by Van Gils et al., Sema3A is of great interest in the goal of remobilizing FCs trapped in atherosclerotic plaques and inducing plaque regression.

2. Hypothesis and aims

2.1. Hypothesis

Sema3A promotes the regression of established atherosclerotic plaques by remobilizing trapped macrophage foam cells.

2.2. Research aims

- 1. To examine the effect of Sema3A on the degree of macrophage migration in vitro.
- 2. To examine the effects of HFD and cholesterol accumulation on the migratory function and phenotype of primary macrophage foam cells, particularly with regards to M1/M2 polarization and expression of the Sema3A receptor Nrp1.
- 3. To determine whether treating mice susceptible to the development of atherosclerosis with super-physiological levels of Sema3A can induce plaque regression, as measured by changes in plaque size and contents.

3. Summary of previous work on Semaphorin 3A in atherosclerosis

The current thesis work is the continuation of a project started by a former PhD student in our lab on the effects of Sema3A on plaque progression in mice²⁷⁶. Many of the methodologies have been carried over to the present project, and will be described in the next section in greater detail. The following is a brief summary of the results, as well as an explanation of the rationale for some of the chosen experiments.

At the onset of HFD and periodically thereafter, ApoE^{-/-} mice were electroporated with a plasmid containing an enhanced green fluorescent protein (eGFP)-Sema3A fusion construct (obtained from de Wit et al.²⁷⁷). This involves injecting a muscle with a DNA plasmid and immediately administering high voltage electrical pulses, which permeabilize the cell membrane for plasmid uptake²⁷⁸ as well as damaging the muscle to promote regeneration and increased protein expression²⁷⁹. Previously, electroporation has been successfully applied to achieve sustained increases in circulating levels of soluble plasmid-encoded proteins²⁸⁰⁻²⁸². Unlike other Semaphorins in vertebrates, class 3 Semaphorins are secreted as opposed to being membrane-associated²²⁷, so plasmid electroporation should, in principle, increase circulating levels of Sema3A and allow it to exert its effect (if any) at sites of atherosclerosis.

Immunofluorescence staining of both atherosclerotic lesions and their healthy vessel counterparts revealed expression of several Sema3A receptors in ECs and macrophages, indicating that these cell types could potentially respond to Sema3A. After confirming elevated Sema3A levels in the plasma using a commercially available enzyme-linked immunosorbent assay (ELISA) kit, it was found that, despite no differences in body weight or serum lipids between the Sema3A and

control (GFP plasmid) conditions, mice that received Sema3A had reduced lesion size and macrophage content, which was associated with a reduced circulating monocyte count. Surprisingly, Sema3A had no effect on monocyte adhesion to VCAM-1 or ICAM-1 in vitro, nor to ECs in an ex vivo perfused (flow-activated) mouse carotid artery. Sema3A also had no effect on monocyte migration, whether in the absence or presence of MCP-1.

A substantial body of evidence suggests that pro-inflammatory, classically activated (M1) macrophages are associated with the progression of atherosclerosis, whereas anti-inflammatory, reparative, alternatively activated (M2) macrophages are associated with plaque regression 283-289. In light of this, cultured M2-polarized macrophages were found to have increased expression of the Sema3A receptor Nrp1 compared to uncommitted (M0) and M1-polarized macrophages. In the presence of Sema3A, Nrp1 expression decreased in the M2 macrophages, presumably by negative feedback regulation; however, Nrp1 expression was still significantly higher than in M0 or M1 macrophages, suggesting that M2 macrophages may be more responsive to Sema3A. Furthermore, Sema3A was found to boost chemoattraction towards MCP-1 in M2- but not M1-polarized macrophages. Altogether, these results suggest that Sema3A reduces atherosclerotic plaque formation by promoting the egress of M2-polarized macrophages from lesions.

In the present study, the effects of Sema3A in atherosclerosis were tested in the context of plaque regression; that is, in lesions that have already fully formed.

4. Materials and methods

4.1. Plasmid information and bacterial preparation

The Sema3A plasmid obtained from De Wit et al.²⁷⁷ contains eGFP inserted between the signal peptide and the Sema domain, allowing direct visualization of the expressed protein. A plasmid containing only GFP was used as a control. Bacteria were transformed with these plasmids, selected for plasmid-specific antibiotic resistance, and grown in broth culture to amplify plasmid copy number. Plasmids were isolated using a commercially available Maxiprep kit and measured by spectrophotometry for concentration and purity.

4.2. Cell line culture, plasmid transfections, and sample collection

To verify the detectability of the eGFP-Sema3A fusion construct, NIH 3T3 cell lines were transfected with the GFP and Sema3A plasmids using the calcium phosphate method²⁹⁰. Cells were removed from liquid nitrogen storage, thawed at room temperature, and allowed to grow in Dulbecco's Modified Eagle Medium (DMEM) supplemented with 10% fetal bovine serum (FBS) and 100U/ml penicillin/streptomycin (1% P/S) in 75 cm² flasks at 37 °C for 72 hours. Cells were then trypsinized, counted, seeded on 6-well plates at a density of 0.4 × 10⁶ cells per well, and allowed to adhere and grow for an additional 24 hours. The culture medium was then replaced and, after three hours, 200 µl of a mixture of plasmid, calcium chloride, and HEPES-buffered saline was added to each well and left to incubate at 37 °C overnight. Culture medium was replaced the following morning to eliminate cytotoxic precipitate. Cells were examined for GFP signal by fluorescence microscopy at 24, 48, and 72 hours post-transfection.

At these time points, 1 ml of conditioned medium was collected from each well, centrifuged at 1,500 rpm at 4 °C for 5 min, and the supernatant was collected and the pellet discarded. After three washes with cold phosphate-buffered saline (PBS) to halt enzymatic activity, 80 µl of a cell lysis buffer containing protease inhibitors was added to each well, and the cells were scraped, collected, sonicated, centrifuged at 15,500 rpm at 4 °C for 15 min, and the supernatant was collected and the pellet discarded. The conditioned medium and cell lysate extracts were stored at -80 °C for analysis at a later date by Western blot (see section 4.10. for protocol) for the presence of GFP or Sema3A protein.

4.3. Mouse handling, high fat diet regimen, and electroporation protocol

ApoE^{-/-} mice of the C57BL/6 strain were obtained from The Jackson Laboratory and bred in the animal facility at the Lady Davis Institute. All personnel involved in handling animals and performing experiments have completed the necessary training modules required by the McGill University Animal Care Committee. Furthermore, all experiments and methods of handling conform to the guidelines set forth by the Animal Care Committee as well as to the protocol of the present research project.

ApoE^{-/-} mice were weaned at four weeks old. At eight weeks old, baseline body weight was obtained and mice were started on HFD (15% cocoa butter fat, 0.5% cholesterol) for nine weeks to allow for sufficient atherosclerotic plaque growth. After re-measuring body weight, one group of mice was euthanized for baseline plaque measurement while the rest were switched back to chow diet and electroporated with either GFP or Sema3A plasmid. Under isoflurane anesthesia, mice were pretreated one hour before administering the plasmid with a 30 μl injection of ~70

μg/ml hyaluronidase in 0.9% NaCl in both quadriceps, which were then massaged to spread out the injected volume. This breaks down the connective tissue surrounding the muscle which can impede effective gene transfer, and has been shown to increase the spatial distribution and overall efficiency of electroporation²⁹¹. Mice were then re-anesthetized by isoflurane and injected in both quadriceps with 50μl of 1μg/μl plasmid (GFP or Sema3A) in 0.9% NaCl and massaged. Immediately following this, a conductive electrolyte gel was applied to the lateral and medial surfaces of both quadriceps, and a series of eight consecutive electrical pulses (200V/cm, 10ms, 1Hz) was delivered through each leg with an electrode clamp.

4.4. Mouse euthanasia and sample collection

Four weeks after electroporation, mice were anesthetized by isoflurane and then euthanized by CO₂ asphyxiation followed by cervical dislocation. Body weight was recorded and cardiac puncture was performed to collect 0.5ml of whole blood in a heparin-coated tube, which was centrifuged at 2,000 rpm at 4 °C for 20 min to collect the plasma. The quadriceps were exposed to ultraviolet light to check for GFP signal, and a piece of GFP-positive muscle was collected, immediately flash frozen in liquid nitrogen, and stored at -80 °C to be homogenized and analyzed by Western blot for the presence of the plasmid-encoded proteins. The whole spleen was weighed and a thin cross section was embedded in optimal cutting temperature (OCT) gel, frozen at -20 °C, and stored at -80 °C to be sectioned at a later date.

The thoracic cage was opened and the heart was flushed with 2% heparin in PBS to rinse the vasculature. Common sites of atherosclerotic plaque growth in mouse models, namely the aortic root, the aortic arch, and the brachiocephalic artery (BCA)^{292,293}, were collected. After removing

other overlying tissues from the exposed thoracic cavity (e.g. lungs, thymus, adipose tissue, vena cava), the major branches of the aorta were cut, and the heart and thoracic aorta were detached together from the posterior wall and intercostal arteries. The BCA was cut from the aortic arch, while the base of the ascending aorta and the ventricles of the heart were cut to collect the aortic root. Both were placed in a 30% sucrose solution at 4 °C for 24 hours to prevent the formation of

paraformaldehyde (PFA) at 4 °C for 24 hours before embedding in OCT gel. As shown in Figure 5, the aortic arch was cut along the greater curvature across the main branches, while the lesser curvature was cut along its entire length, leaving the descending portion of the greater curvature intact. This allows the aortic arch to be folded open for en face staining. The aortic arch was directly fixed in PFA at room temperature for 24 hours and then transferred to 4 °C storage.

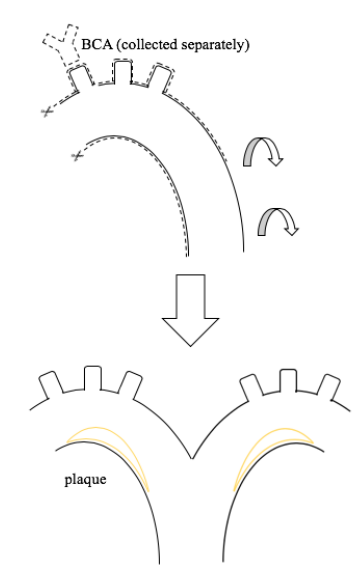


Figure 5: The aortic arch was folded open laterally for en face staining.

4.5. Cryosectioning and tissue staining

OCT-embedded aortic root and BCA samples were serially sectioned into 7 µm slices at -23 °C at tissue depths corresponding to the consistent location of plaques. Several microscope slides were collected from each sample to stain for different markers. Slides were stored at -80 °C until the day of staining and were allowed to thaw at room temperature for 30 min before proceeding. To quantify plaque size, aortic root and BCA sections and PFA-fixed whole aortic arches were stained for 30 min in Oil Red O (ORO) to colorize lipids. Representative light microscope pictures were taken and analyzed by ImageJ, using the polygon selection tool to contour the

plaques. Absolute plaque area was measured using a conversion factor of 542.5 pixels/mm² for the aortic root and 108.5 pixels/mm² for the BCA. For each sample, a single area value was averaged across all pictures. For en face aortic arches, a ratio of plaque area to total arch area (excluding the major branches, down to the ostium of the first intercostal artery) was obtained.

To quantify plaque contents, slides were blocked with 5% bovine serum albumin (BSA) in PBS for 30 min followed by immunofluorescence staining with antibodies targeting common plaque

markers (see Table 1 at the end of Materials and Methods), and captured by fluorescence microscopy. Collagen-I and -III were stained with Sirius Red for 90 min and captured by polarized light microscopy. In ImageJ, threshold analysis was performed on the contoured plaque areas to obtain a percentage of signal-positive area (Figure 6). Once again, these were averaged into a single value per sample.

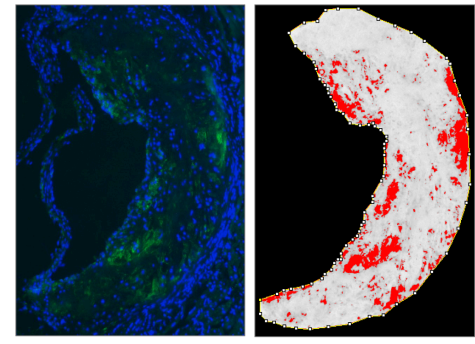


Figure 6: Example of signal threshold analysis, performed by selecting a threshold value such that the signal-positive area within the plaque approximately matches the original immunofluorescence image.

4.6. Extraction and culturing of primary bone marrow-derived monocyte-macrophages

Six to eight weeks old C57BL/6 mice were anesthetized by isoflurane and then euthanized by CO₂ asphyxiation followed by cervical dislocation. Both legs were detached from the pelvis and stripped of their muscle. Under a cell culture hood, the femurs and tibias were cut at both ends and flushed with DMEM + 10% FBS + 1% P/S (using syringes) to collect the bone marrow (BM). BM was pipetted up and down 15 times in a 2 ml glass pipette to physically break it up, and the suspension was then filtered through a 100 μm-pore cell strainer and centrifuged at 1,500 rpm for 5 min. The supernatant was aspirated and the remaining cell pellet was resuspended in

fresh medium, distributed into two 10 cm dishes, and incubated at 37 °C for 1 hour 45 min to allow monocytes to adhere, after which the other non-adherent cells were aspirated²⁹⁴. For the remaining monocytes, DMEM was supplemented with 10% conditioned medium collected from the L929 cell line, which contains M-CSF (among other factors) that promotes the differentiation of monocytes into macrophages^{294,295}. By flow cytometry, L929 conditioned medium was found to generate a similar proportion of BM monocyte-derived macrophages as recombinant M-CSF (85-90% CD11b⁺ F4/80⁺; data not shown). L929-supplemented medium was changed every three days, and after six days the medium was further supplemented with recombinant interleukin-4 (IL-4, 10 ng/ml) for 48 hours to polarize macrophages towards M2²⁹⁶.

4.7. Bone marrow-derived macrophage trans-well migration assay

M2-polarized BM macrophages were starved in low-serum medium (0.5% FBS) for at least four hours prior to the experiment to stop proliferation. Cells were then scraped, counted, and seeded at a density of 100 × 10³ cells per 100 μl into 8 μm-pore trans-well inserts in contact with low-serum medium + 100 ng/ml of recombinant MCP-1 as a chemoattractant in the bottom chamber. Migration was tested under the following four conditions: 1. vehicle (0.1% BSA in PBS); 2. recombinant Sema3A-Fc chimera (100 ng/ml; R&D Systems Cat. 5926-S3); 3. vehicle + p160ROCK inhibitor Y-27632 (10 μM; Tocris Cat. 1254); and 4. Sema3A-Fc + Y-27632. Vehicle or Sema3A was loaded in the bottom well, whereas the inhibitor was loaded with cells in the upper well. Trans-wells were incubated at 37 °C overnight (18 hours) and were checked the following morning for cells that transmigrated across the porous membrane (i.e. attached on the bottom side of the trans-well insert). The upper side of the porous membrane was thoroughly wiped with cotton swabs to eliminate non-migrated cells, and then the trans-wells were fixed in

2% PFA at 37 °C for 15 min. After several washes in PBS to eliminate the PFA, trans-wells were stained in 4',6-diamidino-2-phenylindole (DAPI; 100 ng/ml) for 5 min to stain cell nuclei, and then mounted with the cells facing down. Several fields were captured for each membrane by fluorescence microscopy and cells were counted in ImageJ.

4.8. Bone marrow-derived macrophage RhoA GTPase activation experiments

After six days in culture, primary BM-derived macrophages were immediately scraped, counted, and seeded in 6-well plates with 10 ng/ml of IL-4 at a density of 800×10^6 cells per well for 48 hours to allow cells to re-adhere, proliferate, and polarize towards M2. After serum starving in 0.5% FBS medium for at least four hours, cells were ready for stimulation. In the time-course experiment, cells were stimulated with 100 ng/ml of MCP-1 + 100 ng/ml of Sema3A-Fc for 0 (i.e. nothing added), 5, and 15 min at 37 °C. In a separate experiment, cells were treated with one of four conditions for 5 min: 1. no treatment; 2. MCP-1; 3. Sema3A-Fc; or 4. both. To preserve the active form of the GTPase (RhoA-GTP), cells were quickly processed immediately following stimulation: 6-well plates were placed on ice, rinsed with ice cold PBS, scraped into 50-100 μ l of ice cold lysis buffer provided with the GTPase enzyme-linked immunosorbent assay (G-LISA) kit (Cytoskeleton Cat. BK124), and centrifuged at 10,000 G at 4 °C for 1 min. 10 μ l of supernatant was set aside to measure concentration by spectrophotometry, while the rest was flash frozen in liquid nitrogen and stored at -80 °C. G-LISA was performed according to the protocol included with the kit.

4.9. Peritoneal macrophage and foam cell extraction for migration assays and M1/M2 marker analysis

ApoE^{-/-} mice on either chow diet or HFD for nine weeks received a 1.5 ml peritoneal injection of aged 4% thioglycolate + 100 ng/ml of Sema3A-Fc or vehicle (total of four conditions) to elicit the recruitment of macrophages^{294,297}. In pro-atherogenic mice, these peritoneal macrophages have previously been confirmed to be FCs based on lipid staining²⁹⁸. Four days later, mice were euthanized and macrophages were collected by exposing the peritoneal cavity and injecting and re-aspirating 10 ml of 2% FBS in PBS, taking care not to puncture organs to avoid erythrocyte contamination. Cells were centrifuged at 1,500 rpm for 5 min, re-suspended, and counted before proceeding with experiments.

For quantitative polymerase chain reaction (qPCR) and Western blot analysis of M1 and M2 markers, as well as for trans-well migration assays, peritoneal macrophages were purified by incubating at 37 °C for 1 hour 45 min to allow them to adhere while other cell types would be aspirated out²⁹⁴. Protein was extracted as described for transfected cell lines (section 4.2.; medium not collected) while RNA was extracted using a commercial kit. After measuring RNA concentration and purity by spectrophotometry, genomic DNA was eliminated and the cellular transcriptome was reverse transcribed. cDNA samples were loaded into 96-well PCR plates with primers for M1 (IL-6, Nos2, TNF-α) and M2 markers (Arg1, Retnla, Chil3) as well as for RPS16 as a loading control. Results are presented as fold change between vehicle and Sema3A conditions. Trans-well migration assays were performed as described above (section 4.7), except that these cells had already been stimulated with Sema3A during the thioglycolate injection, and therefore did not require further stimulation with Sema3A directly in the trans-well.

For flow cytometry, 1×10^6 cells were stained with a live/dead marker, blocked with Fc receptor, mixed with antibodies (see Table 1), resuspended in a permeabilization-fixation solution for the intracellular M2 marker Egr2, blocked again with mouse serum, and mixed with anti-Egr2. Samples were centrifuged at 1,500 rpm at 4 °C for 5 min between each step (except between blocking and antibody steps), and all steps up until intracellular blocking and antibody were done on ice (the latter portion was done at room temperature).

4.10. Western blots

All samples were dosed on the day of the Western blot. Depending on the expected band sizes, samples were run on 8, 10, or 15% polyacrylamide gels and then transferred to a nitrocellulose membrane. After rinsing in tris-buffered saline with Tween 20 (TBST), membranes were blocked in 5% skim milk in TBST, followed by the addition of primary antibody in milk (see Table 1 for dilutions and durations). Membranes were again washed in TBST and incubated with secondary antibody in milk. After washing, membranes were covered with an enhanced chemiluminescence solution for 5 min in the dark, inserted into a plastic sleeve, and exposed with a chemiluminescent imaging machine. If required, blotted antibodies were removed with a stripping agent and the membrane was re-blocked and re-blotted with a new primary antibody. Glyceraldehyde 3-phosphate dehydrogenase (GAPDH) or β-actin was blotted as a loading control. All rinsing, blocking, and antibody steps were performed on a rocking platform.

4.11. Statistical methods

In vivo data are presented as mean \pm standard error of mean. Given the variability between experimental runs for in vitro experiments, these values are presented as a ratio of the

experimental condition over the control or vehicle condition to allow pooling of results across different samples and experiment days. Within each experiment, outlier testing was done using the ROUT method (in Prism 6 software). An unpaired, two-tailed T-test was used for experiments with exactly two conditions, whereas a one-way analysis of variance (ANOVA) was used for experiments with more than two conditions. In both cases, the threshold of statistical significance was chosen to be p < 0.05. For statistically significantly results by one-way ANOVA, Tukey's honestly significant difference post-hoc test was used to identify which pair(s) of conditions were significantly different, again at a threshold of p < 0.05. Unless otherwise stated, the post-hoc statistic is presented and not the initial one-way ANOVA statistic. No p-values are presented for preliminary results.

Table 1: List of antibodies used in experiments

Manufacturer (Cat. #)	Host + conjugate	Biological target	Application	Concentration (stock) + conditions
Santa Cruz (sc-9996)	Mouse monoclonal	GFP from Aequorea victoria (jellyfish)	Western blot (primary)	1:1000 (200 µg/ml stock) Overnight at 4 °C
Santa Cruz (sc-74554)	Mouse monoclonal	Sema3A from rat, mouse, human	Western blot (primary)	1:1000 (200 µg/ml stock) Overnight at 4 °C
Cell Signaling Technology (D62C6)	Rabbit monoclonal	Nrp1 from rat, mouse, human	Western blot (primary)	1:1000 (stock concentration not specified) Overnight at 4 °C
Invitrogen (PA3-030A)	Rabbit polyclonal	iNOS from rat, mouse, human + others (M1 marker)	Western blot (primary)	1:2000 (stock concentration not specified) Overnight at 4 °C
Santa Cruz (sc-271430)	Mouse monoclonal	Arg1 from rat, mouse (M2 marker)	Western blot (primary)	1:1000 (200 µg/ml stock) Overnight at 4 °C
Santa Cruz (sc-32233)	Mouse monoclonal	GAPDH from mouse, rat, human, rabbit (loading control)	Western blot (primary)	1:1000 (100 µg/ml stock) 1 hour at room temperature
Santa Cruz (sc-47778)	Mouse monoclonal	β-actin from rat, mouse, human, rabbit + others (loading control)	Western blot (primary)	1:1000 (200 µg/ml stock) 1 hour at room temperature
Biorad (170-6516)	Goat, HRP conjugated	Mouse IgG	Western blot (secondary)	1:2000 (stock concentration not specified) 1 hour at room temperature
Biorad (170-6515)	Goat, HRP conjugated	Rabbit IgG	Western blot (secondary)	1:2000 (stock concentration not specified) 1 hour at room temperature
Santa Cruz (sc-2006)	Goat, HRP conjugated	Rat IgG	Western blot (secondary)	1:2000 (400 µg/ml stock) 1 hour at room temperature

Abcam	Rat monoclonal	Mouse MOMA-	Immuno-	1:50
(ab33451)		(monocyte- macrophage marker)	fluorescence (primary)	(0.5 mg/ml stock) 1 hour at room temperature
Dako (A0452)	Rabbit polyclonal	CD3 from rat, mouse, human + others (T cell marker)	Immuno- fluorescence (primary)	1:100 1 hour at room temperature
BD Biosciences (566387)	Rat monoclonal, PE conjugated	Mouse CD68 (macrophage marker)	Immuno- fluorescence (conjugated)	1:100 (0.2 mg/ml stock) 1 hour at room temperature
Sigma-Aldrich (F3777)	Mouse monoclonal, FITC conjugated	α-SMA from rat, mouse, human + others (SMC marker)	Immuno- fluorescence (conjugated)	1:250 1 hour at room temperature
Invitrogen (A-11006)	Goat polyclonal, AF488 conjugated	Rat IgG	Immuno- fluorescence (secondary)	1:400 (2 mg/ml stock) 1 hour at room temperature
Invitrogen (A-21428)	Goat polyclonal, AF555 conjugated	Rabbit IgG	Immuno- fluorescence (secondary)	1:400 (2 mg/ml stock) 1 hour at room temperature
BioLegend (101227)	Rat monoclonal, PerCP/Cy5.5 conjugated	CD11b from mouse, human (myeloid lineage marker)	Flow cytometry	1:50 (0.2 mg/ml stock) 30 min on ice
BioLegend (135531)	Rat monoclonal, APC/Cy7 conjugated	Mouse CD115 (CD115 ⁺ CD68 ⁻ is a monocyte marker)	Flow cytometry	1:50 (0.2 mg/ml stock) 30 min on ice
BioLegend (108417)	Rat monoclonal, AF488 conjugated	Mouse Gr-1 (granulocytic marker)	Flow cytometry	1:50 (0.5 mg/ml stock) 30 min on ice
BD Biosciences (566387)	Rat monoclonal, PE conjugated	Mouse CD68 (macrophage marker)	Flow cytometry	1:50 (0.2 mg/ml stock) 30 min on ice
BioLegend (102732)	Rat monoclonal, BV421 conjugated	Mouse CD38 (M1 marker)	Flow cytometry	1:150 (0.2 mg/ml stock) 30 min on ice
Invitrogen (17-6691-80)	Rat monoclonal, APC conjugated	Mouse EGR2 (M2 marker)	Flow cytometry	1:50 (0.2 mg/ml stock) 30 min on ice

5. Results

5.1. Transfected cells show no differences between groups by Western blot.

NIH 3T3 fibroblasts were transfected with either control (GFP) or eGFP-Sema3A plasmid and then examined by fluorescence microscopy at 24, 48, and 72 hours.

Consistently across all time points, GFP-transfected cells appeared green while eGFP-Sema3A-transfected cells produced no fluorescent signal. Western blots of the cell lysate and medium extracts revealed distinct band patterns for the anti-GFP and anti-Sema3A antibodies; however, there were no differences between the GFP and Sema3A plasmid conditions (Figure 7).

Nevertheless, these plasmids were used in the electroporation experiments.

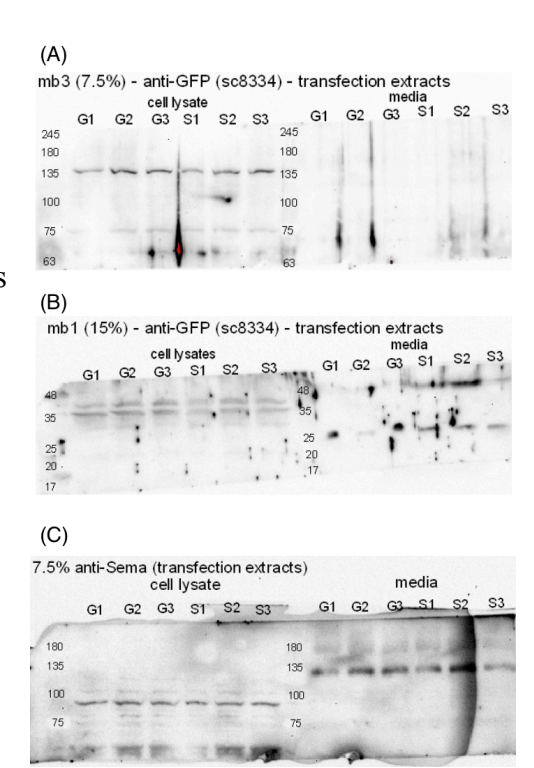
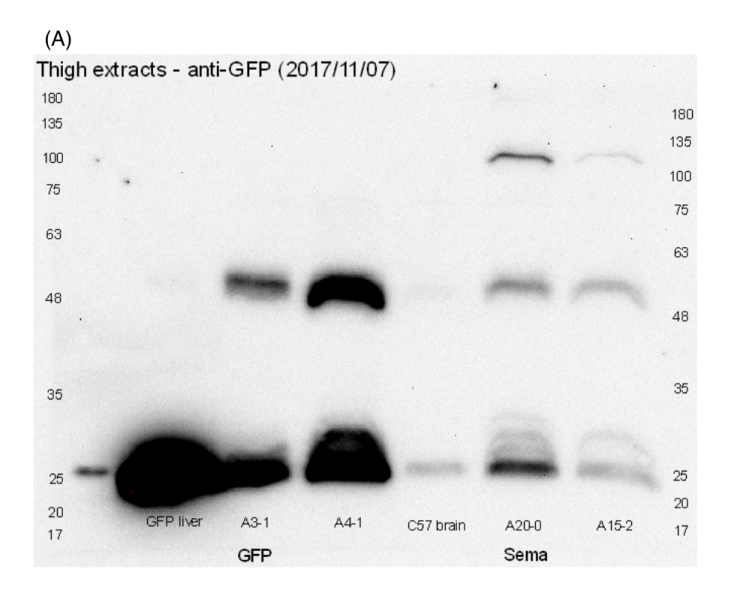


Figure 7: Western blots of cell lysate and medium extracts from NIH 3T3 cells transfected with GFP (G1-3) or Sema3A (S1-3). Blotted with anti-GFP (A, B) and anti-Sema3A antibody (C).

5.2. Electroporated quadriceps show distinct patterns between groups by Western blot.

In contrast to what was observed in the transfected cell lines, protein extracts from quadriceps revealed distinct band patterns between the GFP and Sema3A plasmid conditions. Similar to a GFP-positive control liver extract obtained from GFP knock-in mice, muscle extracts from mice electroporated with the GFP plasmid showed marked overexpression at around 25kDa, which corresponds to the expected band size for GFP (27 kDa). This band was far less expressed in muscle extracts from mice electroporated with the Sema3A plasmid (Figure 8A). Conversely, a much higher molecular weight band (>100 kDa) was uniquely detected in muscle extracts

obtained from mice electroporated with Sema3A, but not GFP plasmid, which also corresponded approximately to a Sema3A-positive control brain extract obtained from C57BL/6 mice (Figure 8B). There was also a very slight but consistent shift in band size between the brain and the Sema3A-electroporated quadriceps extracts, signifying that the exogenously overexpressed, plasmidderived eGFP-Sema3A construct was distinct from the endogenous protein. This was especially evident when blotting with anti-GFP, which revealed the same high molecular weight band (>100 kDa)



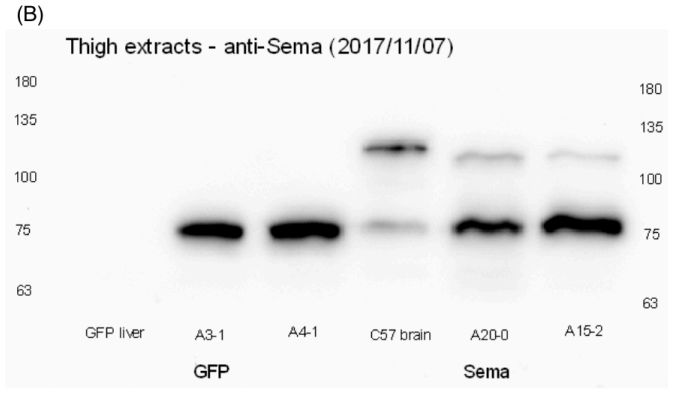


Figure 8: Western blots of protein extracts from quadriceps of atherogenic mice electroporated with GFP or Sema3A plasmid. Blotted with anti-GFP (A) and anti-Sema3A antibody (B).

only for eGFP-Sema-electroporated quadriceps, and neither for GFP-electroporated quadriceps nor for the Sema3A-positive brain extract (Figure 8A). Among eGFP-Sema3A-electroporated mice, only those whose quadriceps produced a fluorescent signal at the injection site (detected using filtered goggles while exciting with ultraviolet light) were subsequently analyzed for plaque size and content.

5.3. Sema3A overexpression does not affect plaque size during regression, but appears to impede a regression-induced increase in plaque collagen.

To see whether overexpressing Sema3A would have an effect on plaque regression, mice were placed on HFD for 9 weeks, after which one group of mice was euthanized for baseline plaque measurements, while the rest returned to a chow diet and were electroporated with either a GFP or eGFP-Sema3A plasmid. Electroporated mice were euthanized four weeks later for plaque analysis. There were no significant differences observed in plaque size between baseline, GFP, and Sema3A conditions. This was true for the aortic arch (Figure 9A) and the aortic root (Figure 9B), and for this reason

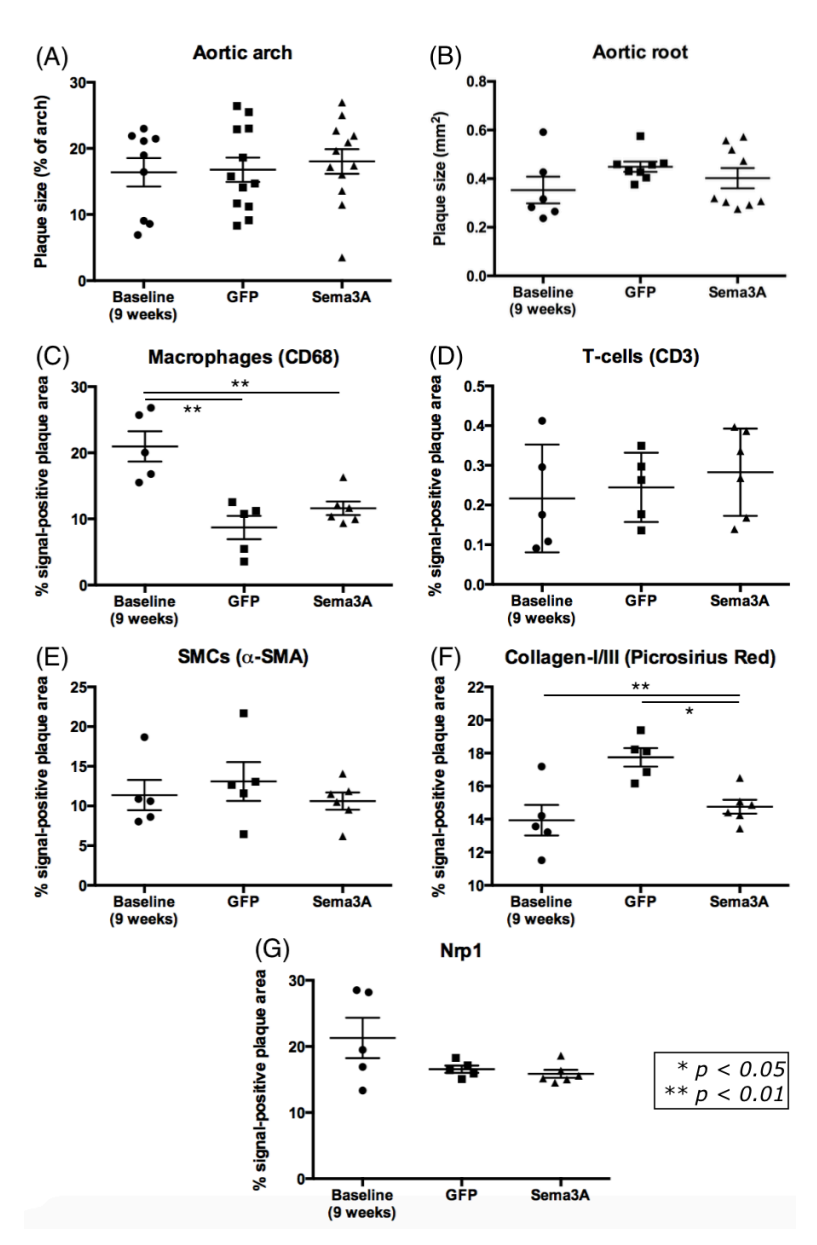


Figure 9: Plaque size in the aortic arch (A) and aortic root (B), and % area composition of macrophages (C), T-cells (D), SMCs (E), collagen-I/III (F), and Nrp1⁺ cells (E) in aortic root plaques at baseline (9 weeks on HFD) and 4 weeks later in mice electroporated with GFP or Sema3A plasmid.

the BCA was not analyzed for plaque size.

Aortic root plaques were further analyzed for their percent composition of common atherosclerotic plaque components. While there was no significant difference in T-cell (Figure 9D) or SMC content (Figure 9E), there was a significant reduction in macrophage content between baseline (Figure 9C; $20.969 \pm 2.288\%$, n = 5) and GFP-treated mice ($8.706 \pm 1.762\%$, n = 5; p = 0.0007) and between baseline and Sema3A-treated mice ($11.623 \pm 1.026\%$, n = 6; p = 0.0044), though there was no significant difference between the GFP and Sema3A conditions. In addition, there was a significant increase in plaque collagen-I/III deposition from baseline (Figure 9F; $13.939 \pm 0.926\%$, n = 5) to four weeks later in GFP-treated mice ($17.746 \pm 0.563\%$, n = 5; p = 0.0037), and this increase was absent in plaques from Sema3A-treated mice ($14.757 \pm 0.563\%$, n = 6; p = 0.0143 for GFP vs. Sema3A). Finally, there was no significant difference in the expression of the Sema3A receptor, Nrp1 (Figure 9G). Overall, these results show that in this diet-dependent mouse model of plaque regression, Sema3A overexpression hinders collagen deposition, but otherwise does not affect plaque size or content.

5.4. Sema3A-induced M2 macrophage chemotaxis is mediated by RhoA signaling

To follow up on our group's previous finding of M2-polarized macrophages having enhanced chemoattraction towards MCP-1 in the presence of Sema3A²⁷⁶, monocytes were extracted from the bone marrow, differentiated into macrophages in the presence of M-CSF-containing medium, polarized towards M2 with IL-4, starved, and tested in a trans-well MCP-1 chemoattraction experiment with or without Y-27632, an inhibitor of ROCK which signals downstream of RhoA GTPase. As shown previously²⁷⁶, Sema3A significantly increases chemoattraction towards MCP-1 by 1.6-fold (Figure 10A; n = 8 for vehicle, n = 7 for Sema3A; p = 0.0348). When the ROCK inhibitor was added on top of this (n = 8), there was no longer an increase in migration

relative to vehicle (p = 0.0044 for Sema3A vs. Sema3A + Y-27632), suggesting that downstream RhoA signaling is what mediates Sema3A-boosted M2 macrophage chemoattraction towards MCP-1.

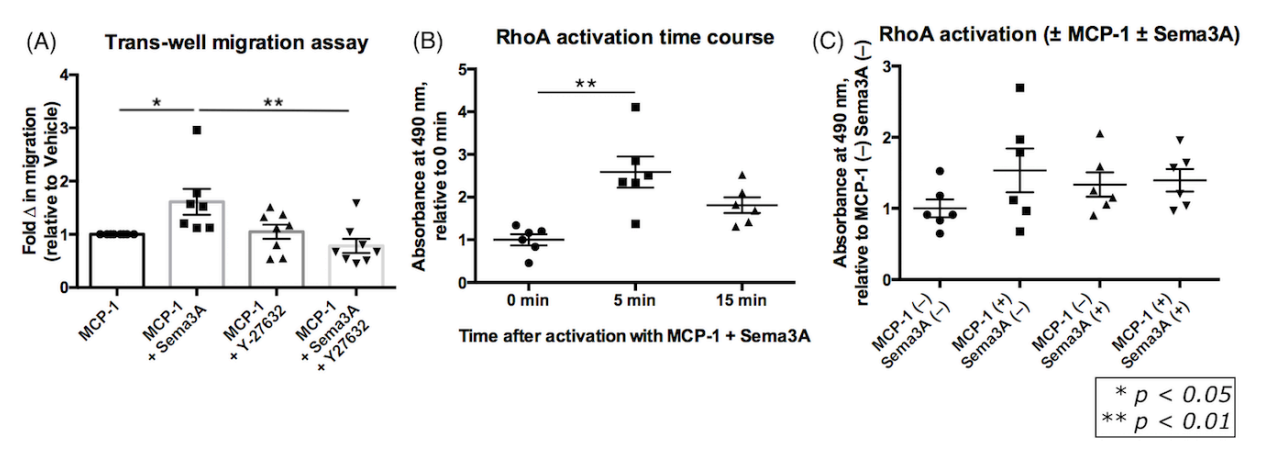


Figure 10: M2-polarized macrophages were tested in trans-well migration (A) and RhoA activation assays (B. time course; C. conditions \pm MCP-1 \pm Sema3A). Data points represent values relative to vehicle for a given experiment.

To verify this, starved M2-polarized macrophages were stimulated with a combination of \pm MCP-1 \pm Sema3A and then rapidly lysed and extracted to determine relative RhoA activity under these various conditions, using a commercial G-LISA plate coated with an antibody that specifically measures the active GTP-bound form (as opposed to the inactive RhoA-GDP). Based on the RhoA activation literature (from a catalogue of various reported stimuli and experimental conditions included with the kit) and a time course experiment involving stimulation with MCP-1 + Sema3A, it was determined that peak activation was achieved at approximately 5 minutes, reaching a 2.5-fold increase in active RhoA (Figure 10B; n = 6 for both 0 min and 5 min; p = 0.0011) and slightly tapering by 15 minutes (1.4-fold decrease vs. 5 min, n = 6; p = 0.0933). Using this time point for peak activity, we next tested for RhoA activation in the four aforementioned conditions (\pm MCP-1 \pm Sema3A). Surprisingly, there was no significant difference found between these conditions (Figure 10C).

5.5. Sema3A promotes foam cell migration selectively in M2-like cells

As the cells that get trapped in lesions, FCs are more relevant to atherosclerosis than non-foamy macrophages. To study the effects of Sema3A on FC phenotype and migration, ApoE^{-/-} mice were placed on either chow diet or HFD for 9 weeks, and then injected intraperitoneally with thioglycolate \pm Sema3A to elicit the recruitment of macrophages/FCs, which were extracted four days later. Among mice on HFD, the addition of Sema3A increased FC recruitment to the peritoneal cavity by over two-fold (Figure 11A; n = 4 for vehicle, n = 5 for Sema3A; p = 0.0049).

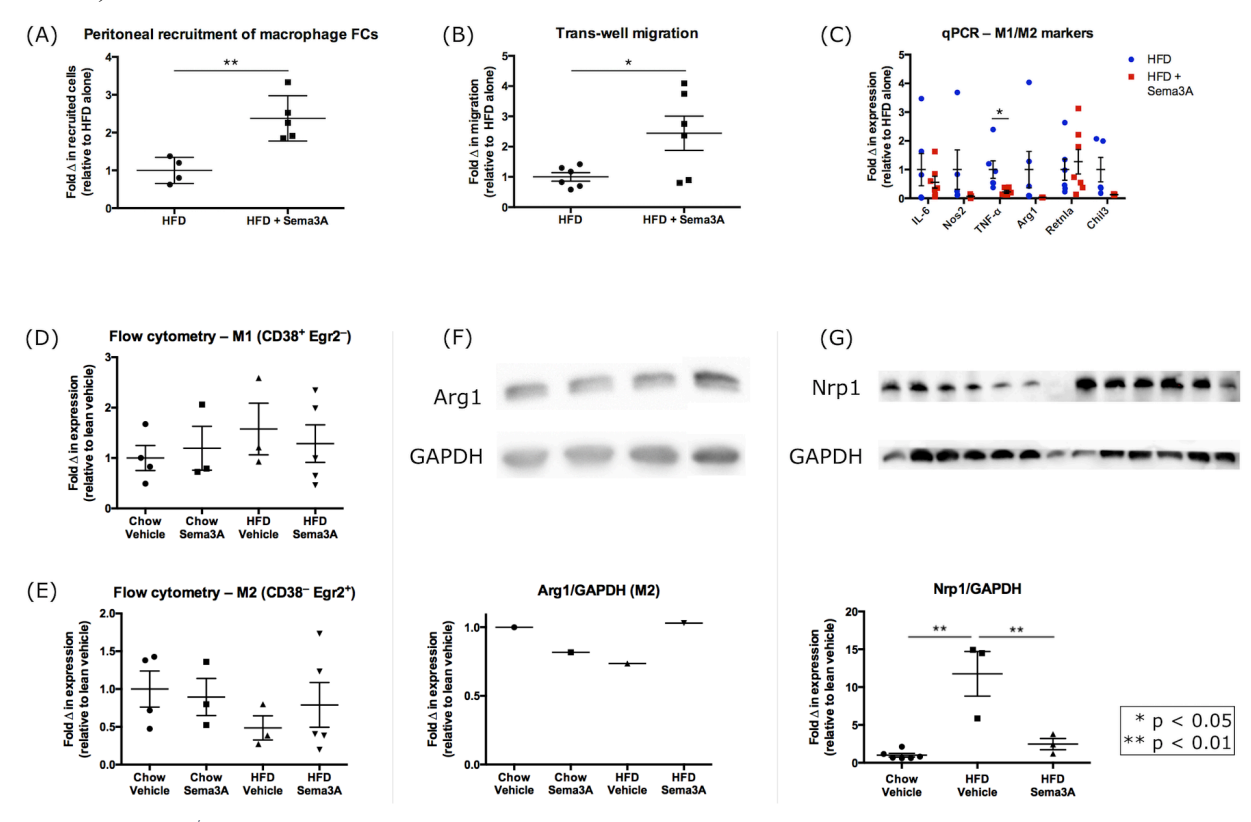


Figure 11: ApoE^{-/-} mice on chow diet or HFD received a peritoneal injection of thioglycolate + vehicle or Sema3A, and then macrophages/FCs were extracted. Conditions were compared in terms of peritoneal cell recruitment (A), trans-well migration (B), and expression of M1 and M2 markers, assessed by qPCR (C), flow cytometry (D, E), and Western blot (F). Nrp1 expression was also compared between conditions by Western blot (G).

Furthermore, when tested in trans-well migration assays, it was found that the Sema3A pretreatment (in the peritoneal cavity) boosted FC chemoattraction towards MCP-1 by 2.4-fold compared to vehicle (Figure 11B; n = 6 for both conditions; p = 0.0330), which is in agreement with the effect observed in BM-derived, M2-polarized macrophages (Figure 10A).

Given our previous finding that Sema3A affects chemotaxis exclusively in M2-polarized, but not M1-polarized or uncommitted macrophages²⁷⁶, peritoneal FCs were assessed by qPCR with a panel of M1 and M2 marker genes to determine whether the Sema3A pre-treatment was selecting for the recruitment of a more M2-like population to the peritoneal cavity. While there was no change in expression for most of the markers tested, Sema3A was found to decrease the expression of the M1 marker TNF-α to 23% of the level found in FCs from mice on HFD alone (Figure 11C, n = 6 for HFD alone, n = 7 for HFD + Sema3A; p = 0.0319). Furthermore, preliminary flow cytometry data suggests that compared to chow diet, the relatively proinflammatory conditions associated with HFD promote an increase in M1-like and a decrease in M2-like cells (Figures 11D, E), and that these trends are attenuated in the presence of Sema3A, which may favour the recruitment of M2-like FCs. Likewise, a preliminary Western blot showed a decrease in expression of the M2 marker Arg1 in peritoneal macrophages/FCs from mice on HFD compared to chow diet, and a significant boost in the presence of Sema3A (Figure 11F). Finally, Western blot revealed a >10-fold boost in the expression of the Sema3A receptor Nrp1 in FCs from mice on HFD compared to chow diet (Figure 11G; n = 6 for chow vehicle vs. n = 3for HFD vehicle; p = 0.0005), and was downregulated in the presence of Sema3A (n = 3, 4.8fold decrease vs. HFD vehicle; p = 0.0038). This is suggestive of a negative feedback mechanism, as was found for Nrp1 expression in BM-derived, M2-polarized macrophages in the presence of Sema3A²⁷⁶. Altogether, these data suggest that in a lipid-rich environment, M2-like macrophage FCs become sensitized to Sema3A stimulation, which boosts their motility.

6. Discussion

Our group previously found that overexpressing Sema3A in pro-atherogenic mice slows the progression of atherosclerosis²⁷⁶. The main difference between the previous work and the present one lies in the timing of plasmid electroporation. In the former, electroporation was concurrent with the onset of HFD and was repeated periodically thereafter. In the latter regression study, electroporation was not administered until after the HFD and plaque progression period. Initially, we tested mice on a continued HFD even after receiving the plasmid, to verify whether Sema3A could induce plaque regression on its own, independent of a return to chow diet. When this was found to not be the case (data not shown), mice were returned to a chow diet at the time of electroporation to see if Sema3A could boost diet-induced plaque regression (with respect to the GFP plasmid).

While Sema3A seemed to prevent an increase in collagen that was observed in the control GFP condition (Figure 9F), in the absence of a similar trend for SMC content (Figure 9E) this should not be interpreted as Sema3A causing a thinning of the fibrous cap during plaque regression. Otherwise, the results show that Sema3A did not affect plaque size (Figure 9A, B) or overall contents (Figure 9C-G). However, it is important to note that even in the GFP condition, there was no reduction in plaque size after switching to chow diet as would be expected. While many established models of plaque regression do involve a switch from HFD to chow diet, this is usually secondary to a more extreme lipid-lowering intervention, such as adenoviral delivery of the human HDL-encoding apoA-I gene²⁰⁷, injection of liposome-forming phospholipids²⁰⁸, and transplantation of lesion-afflicted aortic segments into normolipidemic mice^{272,273}. Before such methods had been conceived, switching to a chow diet was the only way to reliably induce

plaque regression; and even then, this required many months to years to achieve appreciable reductions in plaque size^{184,185,187,299}. In the absence of plaque regression even in the control condition (GFP plasmid), it is difficult to reach any definitive conclusions on the effect of Sema3A overexpression on plaque regression in vivo. A true effect of Sema3A (or lack thereof) on plaque regression would require a more rigorous lipid-lowering strategy as mentioned above, or an extended post-HFD chow diet period.

Another concern was that the mode of delivery, plasmid electroporation, might have failed to achieve the intended overexpression of Sema3A in the mice. While our previous work showed that plasmid electroporation increased plasma Sema3A levels by 80% after one week²⁷⁶, the plasmid was then re-administered every four weeks throughout the plaque development period, so it is possible that circulating Sema3A rose to even greater levels during that time. In the present experiment, only a single dose was administered at the end of the HFD period, so plasma Sema3A levels may not have matched those observed in the former experiment. Furthermore, while Sema3A was detected at the muscular injection site specifically in the Sema3A group and not in the GFP condition (Figure 8), plasma samples could not be tested for Sema3A levels in the present study, for lack of a satisfactory commercially available mouse Sema3A ELISA kit. While we did have an anti-Sema3A antibody that worked for Western blot, attempting to use this in an in-house (non-commercial) ELISA was not successful. Instead, descending thoracic aortas were collected from a subset of electroporated mice to homogenize and detect Sema3A by Western blot near the target site, but again there were no differences between the GFP and Sema3A conditions (data not shown).

Following this, a new mode of delivery was tested: an osmotic pump, which ensures constant release of the loaded protein into the circulation, as opposed to an intravenous injection where protein levels can fluctuate. Structural studies have identified a 15 amino acid-long peptide within Sema3A that interacts with Nrp1³⁰⁰ and induces biological activity comparable to the full-length Sema3A, such as neuronal apoptosis³⁰¹ and inhibition of neurite outgrowth³⁰². The plan was to load this peptide, in parallel with a scrambled sequence peptide as a negative control, into the pumps, rather than the more expensive full-length recombinant protein. However, when the peptide was first tested in trans-well migration assays, it was found to not boost M2 macrophage chemoattraction towards MCP-1 as was the case for the full-length Sema3A (data not shown). Therefore, the osmotic pump delivery method was discontinued.

Beyond the methodological issues encountered, it remains possible that Sema3A only affects plaque progression and not regression. Atherosclerotic plaques are known to contain more M2 macrophages early on, but progressively more M1 macrophages as the disease progresses²⁸³. This, combined with our previous finding that Sema3A increases migration specifically in M2 macrophages²⁷⁶, could possibly explain the lack of an effect on regression: when Sema3A is administered at the onset of atherosclerosis, there are more M2 macrophages present in the early lesions that could immediately experience a boost in migration out of the plaque, which would delay the buildup of lipids, cell debris, and other pro-inflammatory stimuli. In contrast, when the Sema3A treatment is withheld until the plaques have fully formed, the already abundant M1 macrophages might be expected to not respond as well to Sema3A. However, we also found that peritoneal macrophages from mice on HFD had increased expression of Nrp1 compared to those from mice on chow diet (Figure 11G). Therefore, without considering M1/M2 character, one

would expect the same upregulation of Nrp1 in macrophages from late lesions compared to early ones, and that late lesion FCs should be especially responsive to Sema3A. Another finding to consider is that regressing plaques continue to recruit monocytes²²²; in fact, the recruitment of Ly6C^{hi} monocytes is required for the enrichment of M2 macrophages in the plaque and for regression³⁰³. Therefore, Sema3A could potentially act not only on older plaque FCs, but also on newly recruited (especially M2) macrophages. Again, however, the true effects of Sema3A need to be clarified in a more prolonged or aggressive regression model.

As shown previously²⁷⁶, Sema3A boosts M2-polarized macrophage chemoattraction towards MCP-1. Here, this effect was found to depend on RhoA GTPase and its downstream effector p160ROCK, as inhibiting ROCK abrogates this boost (Figure 10A). Using a commercial ELISA kit specific for the active GTP-bound form of RhoA (G-LISA), it was next confirmed that the combined stimulation of M2 macrophages with Sema3A and MCP-1 boosts RhoA activity, peaking around five minutes (Figure 10B). It was therefore surprising that Sema3A was not found to increase RhoA activity on top of MCP-1 alone (Figure 10C), which was expected based on the trans-migration results. However, it is important to note that the boost seen in the time course experiment (Figure 10B) between no stimulation (0 min) and MCP-1 + Sema3A was not present between these same two conditions in the \pm MCP-1 \pm Sema3A experiment (Figure 10C), indicating that the latter experiment may need to be repeated. Aside from the expected boost in RhoA activity by Sema3A on top of MCP-1, one would also expect that in the absence of MCP-1, Sema3A would not induce RhoA. This is based on the finding by our group²⁷⁶ and others ^{224,267,269,274} that Semaphorins specifically affect chemokine-dependent migration, having no effect on their own. Another possibility is that RhoA/ROCK signaling is necessary but not

sufficient for the supplementary effects of Sema3A on M2 macrophage migration when administered in combination with MCP-1, and that other effectors could be at play.

7. Conclusion

To summarize, the present in vivo experiment was not conclusive with regards to the additional effect of Sema3A on atherosclerotic plaque regression, based on the fact that the plasmid overexpression of Sema3A was not measurable in the plasma and that there was no detectable plaque regression even in the control plasmid condition. Beyond these methodological constraints, it remains unclear whether Sema3A could accelerate plaque regression, even in principle alone. While our group previously showed that Sema3A slows down plaque progression, administering Sema3A at the onset of atherogenesis could selectively act on the more M2-like macrophages in the early plaque, which were found to be more sensitive to Sema3A activation based on upregulated Nrp1 receptor. In contrast, when Sema3A treatment is initiated only after plaques have fully formed, the macrophages would be mostly M1-like and would therefore be expected to experience only a minimal boost in migration, if any. Despite this, it should also be considered that Sema3A might act not only on FCs that have been trapped in the plaque from an earlier lesional stage, but also on newly recruited macrophages, which would still have fully intact motility (unencumbered by lipid accumulation) that could be further boosted by Sema3A. Indeed, our in vitro data shows a lot of promise for Sema3A in its ability to selectively recruit M2 macrophages and to boost their migration. Targeted therapies, such as restoring FC motility as was tested in the present body of work, could potentially serve as an effective complementary strategy to the current standard of lipid lowering by statins and lifestyle modifications, with the ultimate end-goal of minimizing cardiovascular morbidity and mortality resulting from atherosclerotic diseases.

8. References

- 1. Heart and Stroke Foundation of Canada. Atherosclerosis [internet]. Ottawa, ON: Heart and Stroke Foundation of Canada; 2018. Available from: https://www.heartandstroke.ca/heart/conditions/atherosclerosis.
- 2. Centers for Disease Control and Prevention (CDC). Coronary Artery Disease (CAD) [internet]. CDC; 2015. Available from: https://www.cdc.gov/heartdisease/coronary_ad.htm.
- 3. Strong JP, Malcom GT, McMahan CA, Tracy RE, Newman WP, 3rd, Herderick EE, et al. Prevalence and extent of atherosclerosis in adolescents and young adults: implications for prevention from the Pathobiological Determinants of Atherosclerosis in Youth Study. JAMA. 1999;281(8):727-35.
- 4. McGill HC, Jr., McMahan CA, Zieske AW, Tracy RE, Malcom GT, Herderick EE, et al. Association of coronary heart disease risk factors with microscopic qualities of coronary atherosclerosis in youth. Circulation. 2000;102(4):374-9.
- 5. Tuzcu EM, Kapadia SR, Tutar E, Ziada KM, Hobbs RE, McCarthy PM, et al. High prevalence of coronary atherosclerosis in asymptomatic teenagers and young adults: evidence from intravascular ultrasound. Circulation. 2001;103(22):2705-10.
- 6. Zinserling WD. Untersuchungen über atherosklerose, 1: über die aortaverfettung bei kindern. Virchows Arch Pathol Anat Physiol Klin Med. 1925;255:677-705.
- 7. Gimbrone MA, Jr., Topper JN, Nagel T, Anderson KR, Garcia-Cardena G. Endothelial dysfunction, hemodynamic forces, and atherogenesis. Ann N Y Acad Sci. 2000;902:230-9.
- 8. Kwak BR, Bäck M, Bochaton-Piallat ML, Caligiuri G, Daemen M, Davies PF, et al. Biomechanical factors in atherosclerosis: mechanisms and clinical implications. Eur Heart J. 2014;35(43):3013-20.
- 9. Malek AM, Alper SL, Izumo S. Hemodynamic shear stress and its role in atherosclerosis. JAMA. 1999;282(21):2035-42.
- 10. Gimbrone MA, Jr. Foreword. In: Lelkes P, editor. Endothelium and mechanical forces. London: Harwood Academic Publishers; 1999. p. VII-IX.
- 11. Cornhill JF, Roach MR. A quantitative study of the localization of atherosclerotic lesions in the rabbit aorta. Atherosclerosis. 1976;23(3):489-501.
- 12. Glagov S, Zarins C, Giddens DP, Ku DN. Hemodynamics and atherosclerosis. Insights and perspectives gained from studies of human arteries. Arch Pathol Lab Med. 1988;112(10):1018-31.
- 13. Steinman DA. Simulated pathline visualization of computed periodic blood flow patterns. J Biomech. 2000;33(5):623-8.
- 14. Soulis JV, Giannoglou GD, Chatzizisis YS, Farmakis TM, Giannakoulas GA, Parcharidis GE, et al. Spatial and phasic oscillation of non-Newtonian wall shear stress in human left coronary artery bifurcation: an insight to atherogenesis. Coron Artery Dis. 2006;17(4):351-8.
- 15. Lee SW, Antiga L, Spence JD, Steinman DA. Geometry of the carotid bifurcation predicts its exposure to disturbed flow. Stroke. 2008;39(8):2341-7.
- 16. Giannoglou GD, Soulis JV, Farmakis TM, Giannakoulas GA, Parcharidis GE, Louridas GE. Wall pressure gradient in normal left coronary artery tree. Med Eng Phys. 2005;27(6):455-64.
- 17. Markl M, Wegent F, Zech T, Bauer S, Strecker C, Schumacher M, et al. In vivo wall shear stress distribution in the carotid artery: effect of bifurcation geometry, internal carotid artery stenosis, and recanalization therapy. Circ Cardiovasc Imaging. 2010;3(6):647-55.

- 18. Dhawan SS, Avati Nanjundappa RP, Branch JR, Taylor WR, Quyyumi AA, Jo H, et al. Shear stress and plaque development. Expert Rev Cardiovasc Ther. 2010;8(4):545-56.
- 19. Nagel T, Resnick N, Dewey CF, Jr., Gimbrone MA, Jr. Vascular endothelial cells respond to spatial gradients in fluid shear stress by enhanced activation of transcription factors. Arterioscler Thromb Vasc Biol. 1999;19(8):1825-34.
- 20. Woolf N. Haemodynamic factors and plaque formation. In: Crawford T, editor. Pathology of atherosclerosis. London: Butterworth Scientific; 1982. p. 187-215.
- 21. Medina A, Suarez de Lezo J, Pan M. Una clasificación simple de las lesiones coronarias en bifurcación. Rev Esp Cardiol. 2006;59(2):183.
- 22. Medina A, Martin P, Suarez de Lezo J, Amador C, Suarez de Lezo J, Pan M, et al. Anatomía vulnerable de la carina en lesiones ostiales de la arteria coronaria descendente anterior tratadas con stent flotante. Rev Esp Cardiol. 2009;62(11):1240-9.
- 23. Nakazawa G, Yazdani SK, Finn AV, Vorpahl M, Kolodgie FD, Virmani R. Pathological findings at bifurcation lesions: the impact of flow distribution on atherosclerosis and arterial healing after stent implantation. J Am Coll Cardiol. 2010;55(16):1679-87.
- 24. van der Giessen AG, Wentzel JJ, Meijboom WB, Mollet NR, van der Steen AF, van de Vosse FN, et al. Plaque and shear stress distribution in human coronary bifurcations: a multislice computed tomography study. EuroIntervention. 2009;4(5):654-61.
- 25. Caro CG, Fitz-Gerald JM, Schroter RC. Atheroma and arterial wall shear. Observation, correlation and proposal of a shear dependent mass transfer mechanism for atherogenesis. Proc R Soc Lond B Biol Sci. 1971;177(1046):109-59.
- 26. Davies PF. Hemodynamic shear stress and the endothelium in cardiovascular pathophysiology. Nat Clin Pract Cardiovasc Med. 2009;6(1):16-26.
- 27. Shaw A, Xu Q. Biomechanical stress-induced signaling in smooth muscle cells: an update. Curr Vasc Pharmacol. 2003;1(1):41-58.
- 28. Ando J, Yamamoto K. Flow detection and calcium signalling in vascular endothelial cells. Cardiovasc Res. 2013;99(2):260-8.
- 29. Tzima E, Irani-Tehrani M, Kiosses WB, Dejana E, Schultz DA, Engelhardt B, et al. A mechanosensory complex that mediates the endothelial cell response to fluid shear stress. Nature. 2005;437(7057):426-31.
- Wang N, Butler JP, Ingber DE. Mechanotransduction across the cell surface and through the cytoskeleton. Science. 1993;260(5111):1124-7.
- 31. Resnick N, Gimbrone MA, Jr. Hemodynamic forces are complex regulators of endothelial gene expression. FASEB J. 1995;9(10):874-82.
- 32. Gimbrone MA, Jr., Nagel T, Topper JN. Biomechanical activation: an emerging paradigm in endothelial adhesion biology. J Clin Invest. 1997;99(8):1809-13.
- 33. Topper JN, Gimbrone MA, Jr. Hemodynamics and endothelial phenotype: new insights into the modulation of vascular gene expression by fluid mechanical stimuli. In: Lelkes P, editor. Endothelium and mechanical forces. London: Harwood Academic Publishers; 1999.
- 34. Chappell DC, Varner SE, Nerem RM, Medford RM, Alexander RW. Oscillatory shear stress stimulates adhesion molecule expression in cultured human endothelium. Circ Res. 1998;82(5):532-9.
- 35. Cuhlmann S, Van der Heiden K, Saliba D, Tremoleda JL, Khalil M, Zakkar M, et al. Disturbed blood flow induces RelA expression via c-Jun N-terminal kinase 1: a novel mode of NF-kappaB regulation that promotes arterial inflammation. Circ Res. 2011;108(8):950-9.

- 36. Xiao H, Lu M, Lin TY, Chen Z, Chen G, Wang WC, et al. Sterol regulatory element binding protein 2 activation of NLRP3 inflammasome in endothelium mediates hemodynamic-induced atherosclerosis susceptibility. Circulation. 2013;128(6):632-42.
- 37. Glagov S, Weisenberg E, Zarins CK, Stankunavicius R, Kolettis GJ. Compensatory enlargement of human atherosclerotic coronary arteries. N Engl J Med. 1987;316(22):1371-5.
- 38. Zarins CK, Zatina MA, Giddens DP, Ku DN, Glagov S. Shear stress regulation of artery lumen diameter in experimental atherogenesis. J Vasc Surg. 1987;5(3):413-20.
- 39. Inaba S, Mintz GS, Shimizu T, Weisz G, Mehran R, Marso SP, et al. Compensatory enlargement of the left main coronary artery: insights from the PROSPECT study. Coron Artery Dis. 2014;25(2):98-103.
- 40. Bevilacqua MP, Pober JS, Mendrick DL, Cotran RS, Gimbrone MA, Jr. Identification of an inducible endothelial-leukocyte adhesion molecule. Proc Natl Acad Sci U S A. 1987;84(24):9238-42.
- 41. Rothlein R, Dustin ML, Marlin SD, Springer TA. A human intercellular adhesion molecule (ICAM-1) distinct from LFA-1. J Immunol. 1986;137(4):1270-4.
- 42. Berliner JA, Territo MC, Sevanian A, Ramin S, Kim JA, Bamshad B, et al. Minimally modified low density lipoprotein stimulates monocyte endothelial interactions. J Clin Invest. 1990;85(4):1260-6.
- 43. Cybulsky MI, Gimbrone MA, Jr. Endothelial expression of a mononuclear leukocyte adhesion molecule during atherogenesis. Science. 1991;251(4995):788-91.
- 44. Nerem RM, Levesque MJ, Cornhill JF. Vascular endothelial morphology as an indicator of the pattern of blood flow. J Biomech Eng. 1981;103(3):172-6.
- 45. Langille BL, O'Donnell F. Reductions in arterial diameter produced by chronic decreases in blood flow are endothelium-dependent. Science. 1986;231(4736):405-7.
- 46. Joris I, Zand T, Majno G. Hydrodynamic injury of the endothelium in acute aortic stenosis. Am J Pathol. 1982;106(3):394-408.
- 47. Walpola PL, Gotlieb AI, Cybulsky MI, Langille BL. Expression of ICAM-1 and VCAM-1 and monocyte adherence in arteries exposed to altered shear stress. Arterioscler Thromb Vasc Biol. 1995;15(1):2-10.
- 48. Zand T, Hoffman AH, Savilonis BJ, Underwood JM, Nunnari JJ, Majno G, et al. Lipid deposition in rat aortas with intraluminal hemispherical plug stenosis. A morphological and biophysical study. Am J Pathol. 1999;155(1):85-92.
- 49. Bussolari SR, Dewey CF, Jr., Gimbrone MA, Jr. Apparatus for subjecting living cells to fluid shear stress. Rev Sci Instrum. 1982;53(12):1851-4.
- 50. Zarins CK, Giddens DP, Bharadvaj BK, Sottiurai VS, Mabon RF, Glagov S. Carotid bifurcation atherosclerosis. Quantitative correlation of plaque localization with flow velocity profiles and wall shear stress. Circ Res. 1983;53(4):502-14.
- 51. Stary HC. Evolution and progression of atherosclerotic lesions in coronary arteries of children and young adults. Arteriosclerosis. 1989;9(1 Suppl):119-32.
- 52. Pflieger HG, K. Konstruktionsprinzipien der aortenwand im ursprungsbereich der interkostalen, intestinalen und renalen aortenäste. Arch Kreislaufforsch. 1970;62:223-48.
- 53. Stehbens WE. Focal intimal proliferation in the cerebral arteries. Am J Pathol. 1960;36:289-301.
- 54. Stehbens WE, Phil D. The renal artery in normal and cholesterol-fed rabbits. Am J Pathol. 1963;43:969-85.

- 55. Wilens SL. The nature of diffuse intimal thickening of arteries. Am J Pathol. 1951;27(5):825-39.
- 56. Movat HZ, More RH, Haust MD. The diffuse intimal thickening of the human aorta with aging. Am J Pathol. 1958;34(6):1023-31.
- 57. Stary HC, Blankenhorn DH, Chandler AB, Glagov S, Insull W, Jr., Richardson M, et al. A definition of the intima of human arteries and of its atherosclerosis-prone regions. A report from the Committee on Vascular Lesions of the Council on Arteriosclerosis, American Heart Association. Circulation. 1992;85(1):391-405.
- 58. Caro CG, Parker KH, Fish PJ, Lever MJ. Blood flow near the arterial wall and arterial disease. Clin Hemor. 1985;5:849-71.
- 59. Glagov SZ, C. K. Is intimal hyperplasia an adaptive response or a pathologic process? Observations on the nature of nonatherosclerotic intimal thickening. J Vasc Surg. 1989;10(5):571-3.
- 60. Schwenke DC, Carew TE. Quantification in vivo of increased LDL content and rate of LDL degradation in normal rabbit aorta occurring at sites susceptible to early atherosclerotic lesions. Circ Res. 1988;62(4):699-710.
- 61. Spring PM, Hoff HF. LDL accumulation in the grossly normal human iliac bifurcation and common iliac arteries. Exp Mol Pathol. 1989;51(2):179-85.
- 62. Getz GS. The involvement of lipoproteins in atherogenesis. Evolving concepts. Ann N Y Acad Sci. 1990;598:17-28.
- 63. Schwenke DC, Carew TE. Initiation of atherosclerotic lesions in cholesterol-fed rabbits. I. Focal increases in arterial LDL concentration precede development of fatty streak lesions. Arteriosclerosis. 1989;9(6):895-907.
- 64. Schwenke DC, Carew TE. Initiation of atherosclerotic lesions in cholesterol-fed rabbits. II. Selective retention of LDL vs. selective increases in LDL permeability in susceptible sites of arteries. Arteriosclerosis. 1989;9(6):908-18.
- 65. Nievelstein PF, Fogelman AM, Mottino G, Frank JS. Lipid accumulation in rabbit aortic intima 2 hours after bolus infusion of low density lipoprotein. A deep-etch and immunolocalization study of ultrarapidly frozen tissue. Arterioscler Thromb. 1991;11(6):1795-805.
- 66. Williams KJ, Tabas I. The response-to-retention hypothesis of early atherogenesis. Arterioscler Thromb Vasc Biol. 1995;15(5):551-61.
- 67. McGill HC, Jr., Geer JC, Holman RL. Sites of vascular vulnerability in dogs demonstrated by Evans blue. AMA Arch Pathol. 1957;64(3):303-11.
- 68. Ross R, Masuda J, Raines EW. Cellular interactions, growth factors, and smooth muscle proliferation in atherogenesis. Ann N Y Acad Sci. 1990;598:102-12.
- 69. Nielsen LB, Nordestgaard BG, Stender S, Kjeldsen K. Aortic permeability to LDL as a predictor of aortic cholesterol accumulation in cholesterol-fed rabbits. Arterioscler Thromb. 1992;12(12):1402-9.
- 70. Thubrikar MJ, Keller AC, Holloway PW, Nolan SP. Distribution of low density lipoprotein in the branch and non-branch regions of the aorta. Atherosclerosis. 1992;97(1):1-9.
- 71. Fry DL, Herderick EE, Johnson DK. Local intimal-medial uptakes of 125I-albumin, 125I-LDL, and parenteral Evans blue dye protein complex along the aortas of normocholesterolemic minipigs as predictors of subsequent hypercholesterolemic atherogenesis. Arterioscler Thromb. 1993;13(8):1193-204.

- 72. Herrmann RA, Malinauskas RA, Truskey GA. Characterization of sites with elevated LDL permeability at intercostal, celiac, and iliac branches of the normal rabbit aorta. Arterioscler Thromb. 1994;14(2):313-23.
- 73. Nordestgaard BG, Nielsen LB. Atherosclerosis and arterial influx of lipoproteins. Curr Opin Lipidol. 1994;5(4):252-7.
- 74. Carew TE, Pittman RC, Marchand ER, Steinberg D. Measurement in vivo of irreversible degradation of low density lipoprotein in the rabbit aorta. Predominance of intimal degradation. Arteriosclerosis. 1984;4(3):214-24.
- 75. Skalen K, Gustafsson M, Rydberg EK, Hulten LM, Wiklund O, Innerarity TL, et al. Subendothelial retention of atherogenic lipoproteins in early atherosclerosis. Nature. 2002;417(6890):750-4.
- 76. Libby P, Ridker PM, Hansson GK. Inflammation in atherosclerosis: from pathophysiology to practice. J Am Coll Cardiol. 2009;54(23):2129-38.
- 77. Steinberg D. Atherogenesis in perspective: hypercholesterolemia and inflammation as partners in crime. Nat Med. 2002;8(11):1211-7.
- 78. Brown MS, Goldstein JL. A receptor-mediated pathway for cholesterol homeostasis. Science. 1986;232(4746):34-47.
- 79. Goldstein JL, Brown MS. Regulation of the mevalonate pathway. Nature. 1990;343(6257):425-30.
- 80. Horton JD, Goldstein JL, Brown MS. SREBPs: activators of the complete program of cholesterol and fatty acid synthesis in the liver. J Clin Invest. 2002;109(9):1125-31.
- 81. Calkin AC, Tontonoz P. Transcriptional integration of metabolism by the nuclear sterolactivated receptors LXR and FXR. Nat Rev Mol Cell Biol. 2012;13(4):213-24.
- 82. Bobryshev YV, Ivanova EA, Chistiakov DA, Nikiforov NG, Orekhov AN. Macrophages and their role in atherosclerosis: pathophysiology and transcriptome analysis. Biomed Res Int. 2016;2016.
- 83. Tall AR, Yvan-Charvet L, Terasaka N, Pagler T, Wang N. HDL, ABC transporters, and cholesterol efflux: implications for the treatment of atherosclerosis. Cell Metab. 2008;7(5):365-75.
- 84. Rothblat GH, Phillips MC. High-density lipoprotein heterogeneity and function in reverse cholesterol transport. Curr Opin Lipidol. 2010;21(3):229-38.
- 85. Chistiakov DA, Bobryshev YV, Orekhov AN. Macrophage-mediated cholesterol handling in atherosclerosis. J Cell Mol Med. 2016;20(1):17-28.
- 86. Tall AR. An overview of reverse cholesterol transport. Eur Heart J. 1998;19 Suppl A:A31-5.
- 87. Gerrity RG. The role of the monocyte in atherogenesis: II. Migration of foam cells from atherosclerotic lesions. Am J Pathol. 1981;103(2):191-200.
- 88. Goldstein JL, Ho YK, Basu SK, Brown MS. Binding site on macrophages that mediates uptake and degradation of acetylated low density lipoprotein, producing massive cholesterol deposition. Proc Natl Acad Sci U S A. 1979;76(1):333-7.
- 89. Lusis AJ. Atherosclerosis. Nature. 2000;407(6801):233-41.
- 90. Yoshida H, Kisugi R. Mechanisms of LDL oxidation. Clin Chim Acta. 2010;411(23-24):1875-82.
- 91. Kunjathoor VV, Febbraio M, Podrez EA, Moore KJ, Andersson L, Koehn S, et al. Scavenger receptors class A-I/II and CD36 are the principal receptors responsible for the uptake

- of modified low density lipoprotein leading to lipid loading in macrophages. J Biol Chem. 2002;277(51):49982-8.
- 92. Yoshida H, Quehenberger O, Kondratenko N, Green S, Steinberg D. Minimally oxidized low-density lipoprotein increases expression of scavenger receptor A, CD36, and macrosialin in resident mouse peritoneal macrophages. Arterioscler Thromb Vasc Biol. 1998;18(5):794-802.
- 93. Nagy L, Tontonoz P, Alvarez JG, Chen H, Evans RM. Oxidized LDL regulates macrophage gene expression through ligand activation of PPARgamma. Cell. 1998;93(2):229-40.
- 94. Suits AG, Chait A, Aviram M, Heinecke JW. Phagocytosis of aggregated lipoprotein by macrophages: low density lipoprotein receptor-dependent foam-cell formation. Proc Natl Acad Sci U S A. 1989;86(8):2713-7.
- 95. Moore KJ, Freeman MW. Scavenger receptors in atherosclerosis: beyond lipid uptake. Arterioscler Thromb Vasc Biol. 2006;26(8):1702-11.
- 96. Elstad MR, La Pine TR, Cowley FS, McEver RP, McIntyre TM, Prescott SM, et al. Pselectin regulates platelet-activating factor synthesis and phagocytosis by monocytes. J Immunol. 1995;155(4):2109-22.
- 97. Weyrich AS, McIntyre TM, McEver RP, Prescott SM, Zimmerman GA. Monocyte tethering by P-selectin regulates monocyte chemotactic protein-1 and tumor necrosis factor-alpha secretion. Signal integration and NF-kappa B translocation. J Clin Invest. 1995;95(5):2297-303.
- 98. Galkina E, Ley K. Vascular adhesion molecules in atherosclerosis. Arterioscler Thromb Vasc Biol. 2007;27(11):2292-301.
- 99. Shih PT, Brennan ML, Vora DK, Territo MC, Strahl D, Elices MJ, et al. Blocking very late antigen-4 integrin decreases leukocyte entry and fatty streak formation in mice fed an atherogenic diet. Circ Res. 1999;84(3):345-51.
- 100. Collins RG, Velji R, Guevara NV, Hicks MJ, Chan L, Beaudet AL. P-Selectin or intercellular adhesion molecule (ICAM)-1 deficiency substantially protects against atherosclerosis in apolipoprotein E-deficient mice. J Exp Med. 2000;191(1):189-94.
- 101. Tacke F, Alvarez D, Kaplan TJ, Jakubzick C, Spanbroek R, Llodra J, et al. Monocyte subsets differentially employ CCR2, CCR5, and CX3CR1 to accumulate within atherosclerotic plaques. J Clin Invest. 2007;117(1):185-94.
- 102. Combadiere C, Potteaux S, Rodero M, Simon T, Pezard A, Esposito B, et al. Combined inhibition of CCL2, CX3CR1, and CCR5 abrogates Ly6C(hi) and Ly6C(lo) monocytosis and almost abolishes atherosclerosis in hypercholesterolemic mice. Circulation. 2008;117(13):1649-57.
- 103. Ley K, Laudanna C, Cybulsky MI, Nourshargh S. Getting to the site of inflammation: the leukocyte adhesion cascade updated. Nat Rev Immunol. 2007;7(9):678-89.
- 104. Gu L, Okada Y, Clinton SK, Gerard C, Sukhova GK, Libby P, et al. Absence of monocyte chemoattractant protein-1 reduces atherosclerosis in low density lipoprotein receptor-deficient mice. Mol Cell. 1998;2(2):275-81.
- 105. Boring L, Gosling J, Cleary M, Charo IF. Decreased lesion formation in CCR2-/- mice reveals a role for chemokines in the initiation of atherosclerosis. Nature. 1998;394(6696):894-7.
- 106. Stary HC. Macrophages, macrophage foam cells, and eccentric intimal thickening in the coronary arteries of young children. Atherosclerosis. 1987;64(2-3):91-108.
- 107. Stary HC, Chandler AB, Glagov S, Guyton JR, Insull W, Jr., Rosenfeld ME, et al. A definition of initial, fatty streak, and intermediate lesions of atherosclerosis. A report from the

- Committee on Vascular Lesions of the Council on Arteriosclerosis, American Heart Association. Arterioscler Thromb. 1994;14(5):840-56.
- 108. Nagao T, Qin C, Grosheva I, Maxfield FR, Pierini LM. Elevated cholesterol levels in the plasma membranes of macrophages inhibit migration by disrupting RhoA regulation. Arterioscler Thromb Vasc Biol. 2007;27(7):1596-602.
- 109. Ridley AJ. Rho GTPases and cell migration. J Cell Sci. 2001;114(Pt 15):2713-22.
- 110. Allen WE, Zicha D, Ridley AJ, Jones GE. A role for Cdc42 in macrophage chemotaxis. J Cell Biol. 1998;141(5):1147-57.
- 111. Yvan-Charvet L, Pagler T, Gautier EL, Avagyan S, Siry RL, Han S, et al. ATP-binding cassette transporters and HDL suppress hematopoietic stem cell proliferation. Science. 2010;328(5986):1689-93.
- 112. Gerrity RG. The role of the monocyte in atherogenesis: I. Transition of blood-borne monocytes into foam cells in fatty lesions. Am J Pathol. 1981;103(2):181-90.
- 113. Lewis JC, Taylor RG, Jerome WG. Foam cell characteristics in coronary arteries and aortas of White Carneau pigeons with moderate hypercholesterolemia. Ann N Y Acad Sci. 1985;454:91-100.
- 114. Quinn MT, Parthasarathy S, Fong LG, Steinberg D. Oxidatively modified low density lipoproteins: a potential role in recruitment and retention of monocyte/macrophages during atherogenesis. Proc Natl Acad Sci U S A. 1987;84(9):2995-8.
- 115. Stary HC. Proliferation of arterial cells in atherosclerosis. Adv Exp Med Biol. 1974;43(0):59-81.
- 116. Stary HC, Malinow MR. Ultrastructure of experimental coronary artery atherosclerosis in cynomolgus macaques. A comparison with the lesions of other primates. Atherosclerosis. 1982;43(2-3):151-75.
- 117. Spraragen SC, Giordano AR, Poon TP, Hamel H. Participation of circulating mononuclear cells in the genesis of atheromata. Circulation. 1969;40(Suppl III):III-24.
- 118. Rosenfeld ME, Ross R. Macrophage and smooth muscle cell proliferation in atherosclerotic lesions of WHHL and comparably hypercholesterolemic fat-fed rabbits. Arteriosclerosis. 1990;10(5):680-7.
- 119. Spraragen SC, Bond VP, Dahl LK. Role of hyperplasia in vascular lesions of cholesterol-fed rabbits studied with thymidine-H3 autoradiography. Circ Res. 1962;11:329-36.
- 120. McMillan GC, Stary HC. Preliminary experience with mitotic activity of cellular elements in the atherosclerotic plaques of cholesterol-fed rabbits studied by labeling with tritiated thymidine. Ann N Y Acad Sci. 1968;149(2):699-709.
- 121. Stary HC, McMillan GC. Kinetics of cellular proliferation in experimental atherosclerosis. Radioautography with grain counts in cholesterol-fed rabbits. Arch Pathol. 1970;89(2):173-83.
- 122. McMillan GC, Duff GL. Mitotic activity in the aortic lesions of experimental cholesterol atherosclerosis of rabbits. Arch Pathol (Chic). 1948;46(2):179-82.
- 123. Gordon D, Reidy MA, Benditt EP, Schwartz SM. Cell proliferation in human coronary arteries. Proc Natl Acad Sci U S A. 1990;87(12):4600-4.
- 124. Tabas I. Apoptosis and plaque destabilization in atherosclerosis: the role of macrophage apoptosis induced by cholesterol. Cell Death Differ. 2004;11 Suppl 1:S12-6.
- 125. Nhan TQ, Liles WC, Schwartz SM. Role of caspases in death and survival of the plaque macrophage. Arterioscler Thromb Vasc Biol. 2005;25(5):895-903.

- 126. Salvayre R, Auge N, Benoist H, Negre-Salvayre A. Oxidized low-density lipoprotein-induced apoptosis. Biochim Biophys Acta. 2002;1585(2-3):213-21.
- 127. Colles SM, Maxson JM, Carlson SG, Chisolm GM. Oxidized LDL-induced injury and apoptosis in atherosclerosis. Potential roles for oxysterols. Trends Cardiovasc Med. 2001;11(3-4):131-8.
- 128. Tabas I. Consequences and therapeutic implications of macrophage apoptosis in atherosclerosis: the importance of lesion stage and phagocytic efficiency. Arterioscler Thromb Vasc Biol. 2005;25(11):2255-64.
- 129. Martinet W, Kockx MM. Apoptosis in atherosclerosis: focus on oxidized lipids and inflammation. Curr Opin Lipidol. 2001;12(5):535-41.
- 130. Zinszner H, Kuroda M, Wang X, Batchvarova N, Lightfoot RT, Remotti H, et al. CHOP is implicated in programmed cell death in response to impaired function of the endoplasmic reticulum. Genes Dev. 1998;12(7):982-95.
- 131. Li G, Mongillo M, Chin KT, Harding H, Ron D, Marks AR, et al. Role of ERO1-alphamediated stimulation of inositol 1,4,5-triphosphate receptor activity in endoplasmic reticulum stress-induced apoptosis. J Cell Biol. 2009;186(6):783-92.
- 132. Timmins JM, Ozcan L, Seimon TA, Li G, Malagelada C, Backs J, et al. Calcium/calmodulin-dependent protein kinase II links ER stress with Fas and mitochondrial apoptosis pathways. J Clin Invest. 2009;119(10):2925-41.
- 133. Seimon T, Tabas I. Mechanisms and consequences of macrophage apoptosis in atherosclerosis. J Lipid Res. 2009;50 Suppl:S382-7.
- 134. Devries-Seimon T, Li Y, Yao PM, Stone E, Wang Y, Davis RJ, et al. Cholesterol-induced macrophage apoptosis requires ER stress pathways and engagement of the type A scavenger receptor. J Cell Biol. 2005;171(1):61-73.
- 135. Gargalovic PS, Gharavi NM, Clark MJ, Pagnon J, Yang WP, He A, et al. The unfolded protein response is an important regulator of inflammatory genes in endothelial cells. Arterioscler Thromb Vasc Biol. 2006;26(11):2490-6.
- 136. Myoishi M, Hao H, Minamino T, Watanabe K, Nishihira K, Hatakeyama K, et al. Increased endoplasmic reticulum stress in atherosclerotic plaques associated with acute coronary syndrome. Circulation. 2007;116(11):1226-33.
- 137. Sanson M, Auge N, Vindis C, Muller C, Bando Y, Thiers JC, et al. Oxidized low-density lipoproteins trigger endoplasmic reticulum stress in vascular cells: prevention by oxygen-regulated protein 150 expression. Circ Res. 2009;104(3):328-36.
- 138. Arai S, Shelton JM, Chen M, Bradley MN, Castrillo A, Bookout AL, et al. A role for the apoptosis inhibitory factor AIM/Spalpha/Api6 in atherosclerosis development. Cell Metab. 2005;1(3):201-13.
- 139. Schrijvers DM, De Meyer GR, Kockx MM, Herman AG, Martinet W. Phagocytosis of apoptotic cells by macrophages is impaired in atherosclerosis. Arterioscler Thromb Vasc Biol. 2005;25(6):1256-61.
- 140. Kockx MM, De Meyer GR, Buyssens N, Knaapen MW, Bult H, Herman AG. Cell composition, replication, and apoptosis in atherosclerotic plaques after 6 months of cholesterol withdrawal. Circ Res. 1998;83(4):378-87.
- 141. van Vlijmen BJ, Gerritsen G, Franken AL, Boesten LS, Kockx MM, Gijbels MJ, et al. Macrophage p53 deficiency leads to enhanced atherosclerosis in APOE*3-Leiden transgenic mice. Circ Res. 2001;88(8):780-6.

- 142. Merched AJ, Williams E, Chan L. Macrophage-specific p53 expression plays a crucial role in atherosclerosis development and plaque remodeling. Arterioscler Thromb Vasc Biol. 2003;23(9):1608-14.
- 143. Liu J, Thewke DP, Su YR, Linton MF, Fazio S, Sinensky MS. Reduced macrophage apoptosis is associated with accelerated atherosclerosis in low-density lipoprotein receptor-null mice. Arterioscler Thromb Vasc Biol. 2005;25(1):174-9.
- 144. Babaev VR, Chew JD, Ding L, Davis S, Breyer MD, Breyer RM, et al. Macrophage EP4 deficiency increases apoptosis and suppresses early atherosclerosis. Cell Metab. 2008;8(6):492-501.
- 145. Boesten LS, Zadelaar AS, van Nieuwkoop A, Hu L, Teunisse AF, Jochemsen AG, et al. Macrophage p53 controls macrophage death in atherosclerotic lesions of apolipoprotein E deficient mice. Atherosclerosis. 2009;207(2):399-404.
- 146. Wang BY, Ho HK, Lin PS, Schwarzacher SP, Pollman MJ, Gibbons GH, et al. Regression of atherosclerosis: role of nitric oxide and apoptosis. Circulation. 1999;99(9):1236-41.
- 147. Kockx MM. Apoptosis in the atherosclerotic plaque: quantitative and qualitative aspects. Arterioscler Thromb Vasc Biol. 1998;18(10):1519-22.
- 148. Steinberg D. Lewis A. Conner Memorial Lecture. Oxidative modification of LDL and atherogenesis. Circulation. 1997;95(4):1062-71.
- 149. Sambrano GR, Steinberg D. Recognition of oxidatively damaged and apoptotic cells by an oxidized low density lipoprotein receptor on mouse peritoneal macrophages: role of membrane phosphatidylserine. Proc Natl Acad Sci U S A. 1995;92(5):1396-400.
- 150. Sambrano GR, Terpstra V, Steinberg D. Independent mechanisms for macrophage binding and macrophage phagocytosis of damaged erythrocytes. Evidence of receptor cooperativity. Arterioscler Thromb Vasc Biol. 1997;17(12):3442-8.
- 151. Chang MK, Bergmark C, Laurila A, Horkko S, Han KH, Friedman P, et al. Monoclonal antibodies against oxidized low-density lipoprotein bind to apoptotic cells and inhibit their phagocytosis by elicited macrophages: evidence that oxidation-specific epitopes mediate macrophage recognition. Proc Natl Acad Sci U S A. 1999;96(11):6353-8.
- 152. Palinski W, Tangirala RK, Miller E, Young SG, Witztum JL. Increased autoantibody titers against epitopes of oxidized LDL in LDL receptor-deficient mice with increased atherosclerosis. Arterioscler Thromb Vasc Biol. 1995;15(10):1569-76.
- 153. Shaw PX, Horkko S, Tsimikas S, Chang MK, Palinski W, Silverman GJ, et al. Humanderived anti-oxidized LDL autoantibody blocks uptake of oxidized LDL by macrophages and localizes to atherosclerotic lesions in vivo. Arterioscler Thromb Vasc Biol. 2001;21(8):1333-9.
- 154. Miller YI, Viriyakosol S, Binder CJ, Feramisco JR, Kirkland TN, Witztum JL. Minimally modified LDL binds to CD14, induces macrophage spreading via TLR4/MD-2, and inhibits phagocytosis of apoptotic cells. J Biol Chem. 2003;278(3):1561-8.
- 155. Henson PM, Bratton DL, Fadok VA. Apoptotic cell removal. Curr Biol. 2001;11(19):R795-805.
- 156. Savill J, Fadok V. Corpse clearance defines the meaning of cell death. Nature. 2000;407(6805):784-8.
- 157. Majno G, Joris I. Apoptosis, oncosis, and necrosis. An overview of cell death. Am J Pathol. 1995;146(1):3-15.
- 158. Mitchinson MJ, Hothersall DC, Brooks PN, De Burbure CY. The distribution of ceroid in human atherosclerosis. J Pathol. 1985;145(2):177-83.

- 159. Ball RY, Stowers EC, Burton JH, Cary NR, Skepper JN, Mitchinson MJ. Evidence that the death of macrophage foam cells contributes to the lipid core of atheroma. Atherosclerosis. 1995;114(1):45-54.
- 160. Fink SL, Cookson BT. Apoptosis, pyroptosis, and necrosis: mechanistic description of dead and dying eukaryotic cells. Infect Immun. 2005;73(4):1907-16.
- 161. Grainger DJ, Reckless J, McKilligin E. Apolipoprotein E modulates clearance of apoptotic bodies in vitro and in vivo, resulting in a systemic proinflammatory state in apolipoprotein E-deficient mice. J Immunol. 2004;173(10):6366-75.
- 162. Schaefer HE. The role of macrophages in atherosclerosis. Haematol Blood Transfus. 1981;27:137-42.
- 163. Libby P, Sukhova G, Lee RT, Galis ZS. Cytokines regulate vascular functions related to stability of the atherosclerotic plaque. J Cardiovasc Pharmacol. 1995;25 Suppl 2:S9-12.
- 164. Taylor PR, Carugati A, Fadok VA, Cook HT, Andrews M, Carroll MC, et al. A hierarchical role for classical pathway complement proteins in the clearance of apoptotic cells in vivo. J Exp Med. 2000;192(3):359-66.
- 165. Vandivier RW, Fadok VA, Hoffmann PR, Bratton DL, Penvari C, Brown KK, et al. Elastase-mediated phosphatidylserine receptor cleavage impairs apoptotic cell clearance in cystic fibrosis and bronchiectasis. J Clin Invest. 2002;109(5):661-70.
- 166. Khan M, Pelengaris S, Cooper M, Smith C, Evan G, Betteridge J. Oxidised lipoproteins may promote inflammation through the selective delay of engulfment but not binding of apoptotic cells by macrophages. Atherosclerosis. 2003;171(1):21-9.
- 167. Li Y, Schwabe RF, DeVries-Seimon T, Yao PM, Gerbod-Giannone MC, Tall AR, et al. Free cholesterol-loaded macrophages are an abundant source of tumor necrosis factor-alpha and interleukin-6: model of NF-kappaB- and map kinase-dependent inflammation in advanced atherosclerosis. J Biol Chem. 2005;280(23):21763-72.
- 168. Stary HC, Chandler AB, Dinsmore RE, Fuster V, Glagov S, Insull W, Jr., et al. A definition of advanced types of atherosclerotic lesions and a histological classification of atherosclerosis. A report from the Committee on Vascular Lesions of the Council on Arteriosclerosis, American Heart Association. Circulation. 1995;92(5):1355-74.
- 169. Timpl R, Dziadek M. Structure, development, and molecular pathology of basement membranes. Int Rev Exp Pathol. 1986;29:1-112.
- 170. Falk E, Nakano M, Bentzon JF, Finn AV, Virmani R. Update on acute coronary syndromes: the pathologists' view. Eur Heart J. 2013;34(10):719-28.
- 171. Libby P. Mechanisms of acute coronary syndromes and their implications for therapy. N Engl J Med. 2013;368(21):2004-13.
- 172. Virmani R, Kolodgie FD, Burke AP, Farb A, Schwartz SM. Lessons from sudden coronary death: a comprehensive morphological classification scheme for atherosclerotic lesions. Arterioscler Thromb Vasc Biol. 2000;20(5):1262-75.
- 173. Ohayon J, Dubreuil O, Tracqui P, Le Floc'h S, Rioufol G, Chalabreysse L, et al. Influence of residual stress/strain on the biomechanical stability of vulnerable coronary plaques: potential impact for evaluating the risk of plaque rupture. Am J Physiol Heart Circ Physiol. 2007;293(3):H1987-96.
- 174. Akyildiz AC, Speelman L, van Brummelen H, Gutierrez MA, Virmani R, van der Lugt A, et al. Effects of intima stiffness and plaque morphology on peak cap stress. Biomed Eng Online. 2011;10:25.

- 175. Cicha I, Worner A, Urschel K, Beronov K, Goppelt-Struebe M, Verhoeven E, et al. Carotid plaque vulnerability: a positive feedback between hemodynamic and biochemical mechanisms. Stroke. 2011;42(12):3502-10.
- 176. de Weert TT, Cretier S, Groen HC, Homburg P, Cakir H, Wentzel JJ, et al. Atherosclerotic plaque surface morphology in the carotid bifurcation assessed with multidetector computed tomography angiography. Stroke. 2009;40(4):1334-40.
- 177. Dirksen MT, van der Wal AC, van den Berg FM, van der Loos CM, Becker AE. Distribution of inflammatory cells in atherosclerotic plaques relates to the direction of flow. Circulation. 1998;98(19):2000-3.
- 178. Gijsen FJ, Wentzel JJ, Thury A, Mastik F, Schaar JA, Schuurbiers JC, et al. Strain distribution over plaques in human coronary arteries relates to shear stress. Am J Physiol Heart Circ Physiol. 2008;295(4):H1608-14.
- 179. Tronc F, Mallat Z, Lehoux S, Wassef M, Esposito B, Tedgui A. Role of matrix metalloproteinases in blood flow-induced arterial enlargement: interaction with NO. Arterioscler Thromb Vasc Biol. 2000;20(12):E120-6.
- 180. Galis ZS, Sukhova GK, Lark MW, Libby P. Increased expression of matrix metalloproteinases and matrix degrading activity in vulnerable regions of human atherosclerotic plaques. J Clin Invest. 1994;94(6):2493-503.
- 181. Vierteljahrschrift für die praktische Heilkunde: Herausgegeben von der medicinischen Facultät in Prag. Erster-sechsunddreissigster Jahrgang. 1844-1879. [Erster]-hundertvierundvierzigster Band: C.L. Hirschfeld (C. Reichenecker); 1856.
- 182. Ignatowski A. Wirkung des tierischen nahrung auf den kaninchenorganismus. Ber Milit Med Akad. 1908;16:154-76.
- 183. Konstantinov IE, Jankovic GM. Alexander I. Ignatowski: a pioneer in the study of atherosclerosis. Tex Heart Inst J. 2013;40(3):246-9.
- 184. Anitschkow N. Uber die veranderungen der kaninchenaorta bei experimenteller cholesterinsteatose. Beitr Path Anat Allg Path. 1913;56:379-404.
- 185. Anitschkow N, Chalatow S. Ueber experimentelle cholester-insteatose und ihre bedeutung fuer die entstehung einiger pathologischer prozesse. Zentrbl Allg Pathol Pathol Anat. 1913;24:1-9.
- 186. Armstrong ML. Evidence of regression of atherosclerosis in primates and man. Postgrad Med J. 1976;52(609):456-61.
- 187. Armstrong ML, Warner ED, Connor WE. Regression of coronary atheromatosis in rhesus monkeys. Circ Res. 1970;27(1):59-67.
- 188. Daoud AS, Jarmolych J, Augustyn JM, Fritz KE. Sequential morphologic studies of regression of advanced atherosclerosis. Arch Pathol Lab Med. 1981;105(5):233-9.
- 189. Feig JE. Regression of atherosclerosis: insights from animal and clinical studies. Ann Glob Health. 2014;80(1):13-23.
- 190. Emini Veseli B, Perrotta P, De Meyer GRA, Roth L, Van der Donckt C, Martinet W, et al. Animal models of atherosclerosis. Eur J Pharmacol. 2017;816:3-13.
- 191. Breslow JL. Mouse models of atherosclerosis. Science. 1996;272(5262):685-8.
- 192. Ishibashi S, Brown MS, Goldstein JL, Gerard RD, Hammer RE, Herz J.
- Hypercholesterolemia in low density lipoprotein receptor knockout mice and its reversal by adenovirus-mediated gene delivery. J Clin Invest. 1993;92(2):883-93.

- 193. Plump AS, Smith JD, Hayek T, Aalto-Setala K, Walsh A, Verstuyft JG, et al. Severe hypercholesterolemia and atherosclerosis in apolipoprotein E-deficient mice created by homologous recombination in ES cells. Cell. 1992;71(2):343-53.
- 194. Zhang SH, Reddick RL, Piedrahita JA, Maeda N. Spontaneous hypercholesterolemia and arterial lesions in mice lacking apolipoprotein E. Science. 1992;258(5081):468-71.
- 195. Mahmood SS, Levy D, Vasan RS, Wang TJ. The Framingham Heart Study and the epidemiology of cardiovascular disease: a historical perspective. Lancet. 2014;383(9921):999-1008.
- 196. Gordon T, Castelli WP, Hjortland MC, Kannel WB, Dawber TR. High density lipoprotein as a protective factor against coronary heart disease. The Framingham Study. Am J Med. 1977;62(5):707-14.
- 197. Keys A, Taylor HL, Blackburn H, Brozek J, Anderson JT, Simonson E. Coronary heart disease among Minnesota business and professional men followed fifteen years. Circulation. 1963;28:381-95.
- 198. Brown MS, Dana SE, Goldstein JL. Regulation of 3-hydroxy-3-methylglutaryl coenzyme A reductase activity in human fibroblasts by lipoproteins. Proc Natl Acad Sci U S A. 1973;70(7):2162-6.
- 199. Goldstein JL, Brown MS. Familial hypercholesterolemia: identification of a defect in the regulation of 3-hydroxy-3-methylglutaryl coenzyme A reductase activity associated with overproduction of cholesterol. Proc Natl Acad Sci U S A. 1973;70(10):2804-8.
- 200. Nathan DG. Cholesterol: the debate should be terminated. FASEB J. 2017;31(7):2722-8.
- 201. Endo A. A historical perspective on the discovery of statins. Proc Jpn Acad Ser B Phys Biol Sci. 2010;86(5):484-93.
- 202. Wissler RW, Vesselinovitch D. Studies of regression of advanced atherosclerosis in experimental animals and man. Ann N Y Acad Sci. 1976;275:363-78.
- 203. Constantinides P. Coronary thrombosis linked to fissure in atherosclerotic vessel wall. JAMA. 1964;188:Suppl:35-7.
- 204. Davies MJ, Richardson PD, Woolf N, Katz DR, Mann J. Risk of thrombosis in human atherosclerotic plaques: role of extracellular lipid, macrophage, and smooth muscle cell content. Br Heart J. 1993;69(5):377-81.
- 205. Badimon JJ, Badimon L, Fuster V. Regression of atherosclerotic lesions by high density lipoprotein plasma fraction in the cholesterol-fed rabbit. J Clin Invest. 1990;85(4):1234-41.
- 206. Miyazaki A, Sakuma S, Morikawa W, Takiue T, Miake F, Terano T, et al. Intravenous injection of rabbit apolipoprotein A-I inhibits the progression of atherosclerosis in cholesterol-fed rabbits. Arterioscler Thromb Vasc Biol. 1995;15(11):1882-8.
- 207. Tangirala RK, Tsukamoto K, Chun SH, Usher D, Pure E, Rader DJ. Regression of atherosclerosis induced by liver-directed gene transfer of apolipoprotein A-I in mice. Circulation. 1999;100(17):1816-22.
- 208. Friedman M, Byers SO, Rosenman RH. Resolution of aortic atherosclerotic infiltration in the rabbit by phosphatide infusion. Proc Soc Exp Biol Med. 1957;95(3):586-8.
- 209. Williams KJ, Feig JE, Fisher EA. Rapid regression of atherosclerosis: insights from the clinical and experimental literature. Nat Clin Pract Cardiovasc Med. 2008;5(2):91-102.
- 210. Nissen SE, Tuzcu EM, Schoenhagen P, Brown BG, Ganz P, Vogel RA, et al. Effect of intensive compared with moderate lipid-lowering therapy on progression of coronary atherosclerosis: a randomized controlled trial. JAMA. 2004;291(9):1071-80.

- 211. Nissen SE, Nicholls SJ, Sipahi I, Libby P, Raichlen JS, Ballantyne CM, et al. Effect of very high-intensity statin therapy on regression of coronary atherosclerosis: the ASTEROID trial. JAMA. 2006;295(13):1556-65.
- 212. Randomised trial of cholesterol lowering in 4444 patients with coronary heart disease: the Scandinavian Simvastatin Survival Study (4S). Lancet. 1994;344(8934):1383-9.
- 213. Newman CB, Preiss D, Tobert JA, Jacobson TA, Page RL, 2nd, Goldstein LB, et al. Statin safety and associated adverse events: a scientific statement from the American Heart Association. Arterioscler Thromb Vasc Biol. 2019;39(2):e38-e81.
- 214. Banach M, Serban MC. Discussion around statin discontinuation in older adults and patients with wasting diseases. J Cachexia Sarcopenia Muscle. 2016;7(4):396-9.
- 215. Jackevicius CA, Mamdani M, Tu JV. Adherence with statin therapy in elderly patients with and without acute coronary syndromes. JAMA. 2002;288(4):462-7.
- 216. Serban MC, Colantonio LD, Manthripragada AD, Monda KL, Bittner VA, Banach M, et al. Statin intolerance and risk of coronary heart events and all-cause mortality following myocardial infarction. J Am Coll Cardiol. 2017;69(11):1386-95.
- 217. Banach M, Stulc T, Dent R, Toth PP. Statin non-adherence and residual cardiovascular risk: there is need for substantial improvement. Int J Cardiol. 2016;225:184-96.
- 218. Ridker PM. C-reactive protein and the prediction of cardiovascular events among those at intermediate risk: moving an inflammatory hypothesis toward consensus. J Am Coll Cardiol. 2007;49(21):2129-38.
- 219. Ridker PM, Cannon CP, Morrow D, Rifai N, Rose LM, McCabe CH, et al. C-reactive protein levels and outcomes after statin therapy. N Engl J Med. 2005;352(1):20-8.
- 220. Ridker PM, Everett BM, Thuren T, MacFadyen JG, Chang WH, Ballantyne C, et al. Antiinflammatory therapy with canakinumab for atherosclerotic disease. N Engl J Med. 2017;377(12):1119-31.
- 221. St Clair RW. Atherosclerosis regression in animal models: current concepts of cellular and biochemical mechanisms. Prog Cardiovasc Dis. 1983;26(2):109-32.
- 222. Llodra J, Angeli V, Liu J, Trogan E, Fisher EA, Randolph GJ. Emigration of monocyte-derived cells from atherosclerotic lesions characterizes regressive, but not progressive, plaques. Proc Natl Acad Sci U S A. 2004;101(32):11779-84.
- 223. van Gils JM, Derby MC, Fernandes LR, Ramkhelawon B, Ray TD, Rayner KJ, et al. The neuroimmune guidance cue netrin-1 promotes atherosclerosis by inhibiting the emigration of macrophages from plaques. Nat Immunol. 2012;13(2):136-43.
- 224. van Gils JM, Ramkhelawon B, Fernandes L, Stewart MC, Guo L, Seibert T, et al. Endothelial expression of guidance cues in vessel wall homeostasis dysregulation under proatherosclerotic conditions. Arterioscler Thromb Vasc Biol. 2013;33(5):911-9.
- 225. Kolodkin AL, Matthes DJ, O'Connor TP, Patel NH, Admon A, Bentley D, et al. Fasciclin IV: sequence, expression, and function during growth cone guidance in the grasshopper embryo. Neuron. 1992;9(5):831-45.
- 226. Luo Y, Raible D, Raper JA. Collapsin: a protein in brain that induces the collapse and paralysis of neuronal growth cones. Cell. 1993;75(2):217-27.
- 227. Kruger RP, Aurandt J, Guan KL. Semaphorins command cells to move. Nat Rev Mol Cell Biol. 2005;6(10):789-800.
- 228. Unified nomenclature for the semaphorins/collapsins. Semaphorin Nomenclature Committee. Cell. 1999;97(5):551-2.

- 229. He Z, Wang KC, Koprivica V, Ming G, Song HJ. Knowing how to navigate: mechanisms of semaphorin signaling in the nervous system. Sci STKE. 2002;2002(119):re1.
- 230. Kolodkin AL, Levengood DV, Rowe EG, Tai YT, Giger RJ, Ginty DD. Neuropilin is a semaphorin III receptor. Cell. 1997;90(4):753-62.
- 231. He Z, Tessier-Lavigne M. Neuropilin is a receptor for the axonal chemorepellent Semaphorin III. Cell. 1997;90(4):739-51.
- 232. Gu C, Yoshida Y, Livet J, Reimert DV, Mann F, Merte J, et al. Semaphorin 3E and plexin-D1 control vascular pattern independently of neuropilins. Science. 2005;307(5707):265-8.
- 233. Raftopoulou M, Hall A. Cell migration: Rho GTPases lead the way. Dev Biol. 2004;265(1):23-32.
- 234. Ridley AJ. Rho GTPase signalling in cell migration. Curr Opin Cell Biol. 2015;36:103-12.
- 235. Ruhrberg C, Schwarz Q. In the beginning: generating neural crest cell diversity. Cell Adh Migr. 2010;4(4):622-30.
- 236. Pasterkamp RJ, Giger RJ. Semaphorin function in neural plasticity and disease. Curr Opin Neurobiol. 2009;19(3):263-74.
- 237. Fawcett JW, Schwab ME, Montani L, Brazda N, Muller HW. Defeating inhibition of regeneration by scar and myelin components. Handb Clin Neurol. 2012;109:503-22.
- 238. Giger RJ, Hollis ER, 2nd, Tuszynski MH. Guidance molecules in axon regeneration. Cold Spring Harb Perspect Biol. 2010;2(7):a001867.
- 239. Gant JC, Thibault O, Blalock EM, Yang J, Bachstetter A, Kotick J, et al. Decreased number of interneurons and increased seizures in neuropilin 2 deficient mice: implications for autism and epilepsy. Epilepsia. 2009;50(4):629-45.
- 240. Yang J, Houk B, Shah J, Hauser KF, Luo Y, Smith G, et al. Genetic background regulates semaphorin gene expression and epileptogenesis in mouse brain after kainic acid status epilepticus. Neuroscience. 2005;131(4):853-69.
- 241. Fujii T, Uchiyama H, Yamamoto N, Hori H, Tatsumi M, Ishikawa M, et al. Possible association of the semaphorin 3D gene (SEMA3D) with schizophrenia. J Psychiatr Res. 2011;45(1):47-53.
- 242. Mah S, Nelson MR, Delisi LE, Reneland RH, Markward N, James MR, et al. Identification of the semaphorin receptor PLXNA2 as a candidate for susceptibility to schizophrenia. Mol Psychiatry. 2006;11(5):471-8.
- 243. Runker AE, O'Tuathaigh C, Dunleavy M, Morris DW, Little GE, Corvin AP, et al. Mutation of Semaphorin-6A disrupts limbic and cortical connectivity and models neurodevelopmental psychopathology. PLoS One. 2011;6(11):e26488.
- 244. Wray NR, James MR, Mah SP, Nelson M, Andrews G, Sullivan PF, et al. Anxiety and comorbid measures associated with PLXNA2. Arch Gen Psychiatry. 2007;64(3):318-26.
- 245. Good PF, Alapat D, Hsu A, Chu C, Perl D, Wen X, et al. A role for semaphorin 3A signaling in the degeneration of hippocampal neurons during Alzheimer's disease. J Neurochem. 2004;91(3):716-36.
- 246. Uchida Y, Ohshima T, Sasaki Y, Suzuki H, Yanai S, Yamashita N, et al. Semaphorin3A signalling is mediated via sequential Cdk5 and GSK3beta phosphorylation of CRMP2: implication of common phosphorylating mechanism underlying axon guidance and Alzheimer's disease. Genes Cells. 2005;10(2):165-79.

- 247. Clarimon J, Scholz S, Fung HC, Hardy J, Eerola J, Hellstrom O, et al. Conflicting results regarding the semaphorin gene (SEMA5A) and the risk for Parkinson disease. Am J Hum Genet. 2006;78(6):1082-4; author reply 92-4.
- 248. Maraganore DM, de Andrade M, Lesnick TG, Strain KJ, Farrer MJ, Rocca WA, et al. High-resolution whole-genome association study of Parkinson disease. Am J Hum Genet. 2005;77(5):685-93.
- 249. Kotter MR, Stadelmann C, Hartung HP. Enhancing remyelination in disease—can we wrap it up? Brain. 2011;134(Pt 7):1882-900.
- 250. Serini G, Valdembri D, Zanivan S, Morterra G, Burkhardt C, Caccavari F, et al. Class 3 semaphorins control vascular morphogenesis by inhibiting integrin function. Nature. 2003;424(6947):391-7.
- 251. Zygmunt T, Gay CM, Blondelle J, Singh MK, Flaherty KM, Means PC, et al. Semaphorin-PlexinD1 signaling limits angiogenic potential via the VEGF decoy receptor sFlt1. Dev Cell. 2011;21(2):301-14.
- 252. Tse C, Xiang RH, Bracht T, Naylor SL. Human Semaphorin 3B (SEMA3B) located at chromosome 3p21.3 suppresses tumor formation in an adenocarcinoma cell line. Cancer Res. 2002;62(2):542-6.
- 253. Xiang R, Davalos AR, Hensel CH, Zhou XJ, Tse C, Naylor SL. Semaphorin 3F gene from human 3p21.3 suppresses tumor formation in nude mice. Cancer Res. 2002;62(9):2637-43.
- 254. Sekido Y, Bader S, Latif F, Chen JY, Duh FM, Wei MH, et al. Human semaphorins A(V) and IV reside in the 3p21.3 small cell lung cancer deletion region and demonstrate distinct expression patterns. Proc Natl Acad Sci U S A. 1996;93(9):4120-5.
- 255. Zabarovsky ER, Lerman MI, Minna JD. Tumor suppressor genes on chromosome 3p involved in the pathogenesis of lung and other cancers. Oncogene. 2002;21(45):6915-35.
- 256. Tomizawa Y, Sekido Y, Kondo M, Gao B, Yokota J, Roche J, et al. Inhibition of lung cancer cell growth and induction of apoptosis after reexpression of 3p21.3 candidate tumor suppressor gene SEMA3B. Proc Natl Acad Sci U S A. 2001;98(24):13954-9.
- 257. Castro-Rivera E, Ran S, Thorpe P, Minna JD. Semaphorin 3B (SEMA3B) induces apoptosis in lung and breast cancer, whereas VEGF165 antagonizes this effect. Proc Natl Acad Sci U S A. 2004;101(31):11432-7.
- 258. Bielenberg DR, Hida Y, Shimizu A, Kaipainen A, Kreuter M, Kim CC, et al. Semaphorin 3F, a chemorepulsant for endothelial cells, induces a poorly vascularized, encapsulated, nonmetastatic tumor phenotype. J Clin Invest. 2004;114(9):1260-71.
- 259. Boyce BF, Xing L. Functions of RANKL/RANK/OPG in bone modeling and remodeling. Arch Biochem Biophys. 2008;473(2):139-46.
- 260. Hayashi M, Nakashima T, Taniguchi M, Kodama T, Kumanogoh A, Takayanagi H. Osteoprotection by semaphorin 3A. Nature. 2012;485(7396):69-74.
- 261. Fukuda T, Takeda S, Xu R, Ochi H, Sunamura S, Sato T, et al. Sema3A regulates bonemass accrual through sensory innervations. Nature. 2013;497(7450):490-3.
- 262. Dacquin R, Starbuck M, Schinke T, Karsenty G. Mouse alpha1(I)-collagen promoter is the best known promoter to drive efficient Cre recombinase expression in osteoblast. Dev Dyn. 2002;224(2):245-51.
- 263. Rodda SJ, McMahon AP. Distinct roles for Hedgehog and canonical Wnt signaling in specification, differentiation and maintenance of osteoblast progenitors. Development. 2006;133(16):3231-44.

- 264. Suto F, Ito K, Uemura M, Shimizu M, Shinkawa Y, Sanbo M, et al. Plexin-a4 mediates axon-repulsive activities of both secreted and transmembrane semaphorins and plays roles in nerve fiber guidance. J Neurosci. 2005;25(14):3628-37.
- 265. Lepelletier Y, Moura IC, Hadj-Slimane R, Renand A, Fiorentino S, Baude C, et al. Immunosuppressive role of semaphorin-3A on T cell proliferation is mediated by inhibition of actin cytoskeleton reorganization. Eur J Immunol. 2006;36(7):1782-93.
- 266. Lepelletier Y, Smaniotto S, Hadj-Slimane R, Villa-Verde DM, Nogueira AC, Dardenne M, et al. Control of human thymocyte migration by Neuropilin-1/Semaphorin-3A-mediated interactions. Proc Natl Acad Sci U S A. 2007;104(13):5545-50.
- 267. Takamatsu H, Takegahara N, Nakagawa Y, Tomura M, Taniguchi M, Friedel RH, et al. Semaphorins guide the entry of dendritic cells into the lymphatics by activating myosin II. Nat Immunol. 2010;11(7):594-600.
- 268. Catalano A. The neuroimmune semaphorin-3A reduces inflammation and progression of experimental autoimmune arthritis. J Immunol. 2010;185(10):6373-83.
- 269. Rienks M, Carai P, Bitsch N, Schellings M, Vanhaverbeke M, Verjans J, et al. Sema3A promotes the resolution of cardiac inflammation after myocardial infarction. Basic Res Cardiol. 2017;112(4):42.
- 270. Zhu L, Stalker TJ, Fong KP, Jiang H, Tran A, Crichton I, et al. Disruption of SEMA4D ameliorates platelet hypersensitivity in dyslipidemia and confers protection against the development of atherosclerosis. Arterioscler Thromb Vasc Biol. 2009;29(7):1039-45.
- 271. Yukawa K, Tanaka T, Kishino M, Yoshida K, Takeuchi N, Ito T, et al. Deletion of Sema4D gene reduces intimal neovascularization and plaque growth in apolipoprotein E-deficient mice. Int J Mol Med. 2010;26(1):39-44.
- 272. Reis ED, Li J, Fayad ZA, Rong JX, Hansoty D, Aguinaldo JG, et al. Dramatic remodeling of advanced atherosclerotic plaques of the apolipoprotein E-deficient mouse in a novel transplantation model. J Vasc Surg. 2001;34(3):541-7.
- 273. Chereshnev I, Trogan E, Omerhodzic S, Itskovich V, Aguinaldo JG, Fayad ZA, et al. Mouse model of heterotopic aortic arch transplantation. J Surg Res. 2003;111(2):171-6.
- 274. Wanschel A, Seibert T, Hewing B, Ramkhelawon B, Ray TD, van Gils JM, et al. Neuroimmune guidance cue Semaphorin 3E is expressed in atherosclerotic plaques and regulates macrophage retention. Arterioscler Thromb Vasc Biol. 2013;33(5):886-93.
- 275. Hu S, Liu Y, You T, Heath J, Xu L, Zheng X, et al. Vascular Semaphorin 7A upregulation by disturbed flow promotes atherosclerosis through endothelial $\beta 1$ Integrin. Arterioscler Thromb Vasc Biol. 2017.
- 276. Heidari M. Semaphorin-3A, a regulator of the immune system [dissertation]. Montreal, QC: McGill University; 2016.
- 277. De Wit J, De Winter F, Klooster J, Verhaagen J. Semaphorin 3A displays a punctate distribution on the surface of neuronal cells and interacts with proteoglycans in the extracellular matrix. Mol Cell Neurosci. 2005;29(1):40-55.
- 278. Andre F, Mir LM. DNA electrotransfer: its principles and an updated review of its therapeutic applications. Gene Ther. 2004;11 Suppl 1:S33-42.
- 279. Vitadello M, Schiaffino MV, Picard A, Scarpa M, Schiaffino S. Gene transfer in regenerating muscle. Hum Gene Ther. 1994;5(1):11-8.
- 280. Aihara H, Miyazaki J. Gene transfer into muscle by electroporation in vivo. Nat Biotechnol. 1998;16(9):867-70.

- 281. Kreiss P, Bettan M, Crouzet J, Scherman D. Erythropoietin secretion and physiological effect in mouse after intramuscular plasmid DNA electrotransfer. J Gene Med. 1999;1(4):245-50.
- 282. Eefting D, de Vries MR, Grimbergen JM, Karper JC, van Bockel JH, Quax PH. In vivo suppression of vein graft disease by nonviral, electroporation-mediated, gene transfer of tissue inhibitor of metalloproteinase-1 linked to the amino terminal fragment of urokinase (TIMP-1.ATF), a cell-surface directed matrix metalloproteinase inhibitor. J Vasc Surg. 2010;51(2):429-37.
- 283. Khallou-Laschet J, Varthaman A, Fornasa G, Compain C, Gaston AT, Clement M, et al. Macrophage plasticity in experimental atherosclerosis. PLoS One. 2010;5(1):e8852.
- 284. Feig JE, Parathath S, Rong JX, Mick SL, Vengrenyuk Y, Grauer L, et al. Reversal of hyperlipidemia with a genetic switch favorably affects the content and inflammatory state of macrophages in atherosclerotic plaques. Circulation. 2011;123(9):989-98.
- 285. Feig JE, Rong JX, Shamir R, Sanson M, Vengrenyuk Y, Liu J, et al. HDL promotes rapid atherosclerosis regression in mice and alters inflammatory properties of plaque monocytederived cells. Proc Natl Acad Sci U S A. 2011;108(17):7166-71.
- 286. Rayner KJ, Sheedy FJ, Esau CC, Hussain FN, Temel RE, Parathath S, et al. Antagonism of miR-33 in mice promotes reverse cholesterol transport and regression of atherosclerosis. J Clin Invest. 2011;121(7):2921-31.
- 287. Chinetti-Gbaguidi G, Baron M, Bouhlel MA, Vanhoutte J, Copin C, Sebti Y, et al. Human atherosclerotic plaque alternative macrophages display low cholesterol handling but high phagocytosis because of distinct activities of the PPARgamma and LXRalpha pathways. Circ Res. 2011;108(8):985-95.
- 288. Chistiakov DA, Bobryshev YV, Nikiforov NG, Elizova NV, Sobenin IA, Orekhov AN. Macrophage phenotypic plasticity in atherosclerosis: the associated features and the peculiarities of the expression of inflammatory genes. Int J Cardiol. 2015;184:436-45.
- 289. de Gaetano M, Crean D, Barry M, Belton O. M1- and M2-type macrophage responses are predictive of adverse outcomes in human atherosclerosis. Front Immunol. 2016;7:275.
- 290. Kingston RE, Chen CA, Rose JK. Calcium phosphate transfection. Curr Protoc Mol Biol. 2003;63(1).
- 291. McMahon JM, Signori E, Wells KE, Fazio VM, Wells DJ. Optimisation of electrotransfer of plasmid into skeletal muscle by pretreatment with hyaluronidase increased expression with reduced muscle damage. Gene Ther. 2001;8(16):1264-70.
- 292. Bond AR, Jackson CL. The fat-fed apolipoprotein E knockout mouse brachiocephalic artery in the study of atherosclerotic plaque rupture. J Biomed Biotechnol. 2011;2011:379069.
- 293. VanderLaan PA, Reardon CA, Getz GS. Site specificity of atherosclerosis: site-selective responses to atherosclerotic modulators. Arterioscler Thromb Vasc Biol. 2004;24(1):12-22.
- 294. Zhang X, Goncalves R, Mosser DM. The isolation and characterization of murine macrophages. Curr Protoc Immunol. 2008;83(1).
- 295. Austin PE, McCulloch EA, Till JE. Characterization of the factor in L-cell conditioned medium capable of stimulating colony formation by mouse marrow cells in culture. J Cell Physiol. 1971;77(2):121-34.
- 296. Stein M, Keshav S, Harris N, Gordon S. Interleukin 4 potently enhances murine macrophage mannose receptor activity: a marker of alternative immunologic macrophage activation. J Exp Med. 1992;176(1):287-92.

- 297. Li YM, Baviello G, Vlassara H, Mitsuhashi T. Glycation products in aged thioglycollate medium enhance the elicitation of peritoneal macrophages. J Immunol Methods. 1997;201(2):183-8.
- 298. Li AC, Binder CJ, Gutierrez A, Brown KK, Plotkin CR, Pattison JW, et al. Differential inhibition of macrophage foam-cell formation and atherosclerosis in mice by PPARalpha, beta/delta, and gamma. J Clin Invest. 2004;114(11):1564-76.
- 299. Maruffo CA, Portman OW. Nutritional control of coronary artery atherosclerosis in the squirrel monkey. J Atheroscler Res. 1968;8(2):237-47.
- 300. Ueyama H, Horibe T, Nakajima O, Ohara K, Kohno M, Kawakami K. Semaphorin 3A lytic hybrid peptide binding to neuropilin-1 as a novel anti-cancer agent in pancreatic cancer. Biochem Biophys Res Commun. 2011;414(1):60-6.
- 301. Shirvan A, Shina R, Ziv I, Melamed E, Barzilai A. Induction of neuronal apoptosis by Semaphorin3A-derived peptide. Brain Res Mol Brain Res. 2000;83(1-2):81-93.
- 302. Kohno M, Ohara K, Horibe T, Kawakami K. Inhibition of neurite outgrowth by a Neuropilin-1 binding peptide derived from Semaphorin 3A. Int J Pept Res Ther. 2014;20(2):153-60.
- 303. Rahman K, Vengrenyuk Y, Ramsey SA, Vila NR, Girgis NM, Liu J, et al. Inflammatory Ly6C(hi) monocytes and their conversion to M2 macrophages drive atherosclerosis regression. J Clin Invest. 2017;127(8):2904-15.